FOSSIL

DOE/PC/90293--T15
(DE95009310)

HIGH-TEMPERATURE MEMBRANES FOR H_2S AND SO_2 SEPARATIONS

Final Report

By
J. Winnick

January 1995

Work Performed Under Contract No. FG22-90PC90293

For
U.S. Department of Energy
Pittsburgh Energy Technology Center
Pittsburgh, Pennsylvania

By
Georgia Institute of Technology
Atlanta, Georgia

MASTER

DISCLAIMER

DOE/PC/90293--T15
(DE95009310)
Distribution Category UC-113

HIGH-TEMPERATURE MEMBRANES FOR H_2S AND SO_2 SEPARATIONS

DE-FG22-90PC90293

FINAL REPORT

JANUARY 1995

Georgia Institute of Technology
Jack Winnick, P.I.

Table of Contents

List of Figures

List of Tables

EXECUTIVE SUMMARY

Electrochemical cells which separate H_2S and SO_2 from hot gas streams have two important materials issues that limit their successful industrial application: (1) membranes and (2) electrodes. These were the focus of the present study.

For the H_2S work, experimental analysis incorporated several membrane and electrode materials; densified zirconia provided the best matrices for entrainment of electrolytic species, ionic mobility, and a process-gas barricade hindering the capabilities of gas cross-over, alternate reactions. In-lab densification of a zirconia weave/knit mat using sub-micron particles of zirconia in an aqueous suspension provided the most efficient and economical manufacturing technique. Electrode materials of lithiated Ni converted to NiO in-situ were successful in polishing applications; however H_2S levels > 100 ppm converted the NiO cathode to a molten nickel sulfide necessitating the use of Co. Lithiated NiO for the anode material remained morphologically stable and conductive in all experimentation.

High temperature electrochemical removal of H_2S from coal gasification streams has been shown on the bench scale level at the Georgia Institute of Technology utilizing the aforementioned materials. Experimental removals from 1000 ppm to 100 ppm H_2S and 100 ppm to 10 ppm H_2S proved over 90% removal with applied current was economically feasible due to high current efficiencies (~100%) and low polarizations; therefore low power requirements for removal applications in the above ranges. Polishing of H_2S from 10 ppm to < 1 ppm tested the most stringent application of the

electrochemical cell due to the low concentration of H_2S compared to CO_2. Removals over 90% were achieved; power requirements for this level of removal are negligible.

For the SO_2 work, an extensive search was conducted for a suitable membrane material for use in the SO_2 removal system. The most favorable material found was Si_3N_4, proven to be more efficient than other possible materials. In addition, tape casting was proven to be the method of choice for delivery of the ceramic matrix in full cell testing. New lithiated NiO electrodes were also developed and characterized, proving more stable than previously used pervoskite electrodes.

The combination of these new components led to 90% removal at near 100% current efficiency over a wide range of current densities. Cells proved highly stable over the unprecedented period of 30 days, showing identical characteristics from beginning to end of experimentation.

The highest levels of current density are commensurate with economic cell design; they are limited only by mass-transfer from the bulk gas, as expected from modeling of the system. With the high current densities tested, SO_2 generation was observed at the cathode due to chemical and electrochemical complications. This generation was characterized with respect to O_2 partial pressure. Electrodes with higher reaction area were being tested for the ability to eliminate this limitation as the research period ended.

INTRODUCTION

Use of selective membranes for separating gaseous components from mixtures is experiencing escalating interest. Most rely on a pressure or concentration difference to provide a chemical potential driving force:

$$\Delta\mu_i = \mu_i - \mu'_i = RT \ln (a_i / a'_i) \quad (1)$$

where the activities of component *i* in the two phases separated by the membrane are noted a_i and a'_i. Facilitated transport through a chemical or surface reaction can sometimes be employed to aid selectivity and permeability. In certain instances, an electric field can be employed as an alternative. For species with a net charge, z_i, the driving force across a membrane becomes the electrochemical potential difference, $\Delta\bar{\mu}_i$:

$$\Delta\bar{\mu}_i = \bar{\mu}_i - \bar{\mu}'_i = RT \ln(a_i / a'_i) + z_i F \Delta\Phi \quad (2)$$

where $\Delta\Phi$ is the potential difference across the membrane.

The simplest application of this technique is the preparation of nearly pure oxygen from air[1]. An asbestos mat or a few sheets of filter paper, soaked in aqueous KOH (electrolyte) serves as the membrane. The electric field is created by a low voltage DC power supply (or battery) attached across two nickel screens (or porous electrodes) pressed to either side of the membrane. Air passes by the negative screen (cathode) where oxygen is reduced:

$$1/2\ O_2 + H_2O + 2\ e^- \Rightarrow 2\ OH^- \quad (3)$$

At the positive screen (anode), hydroxide is oxidized:

$$2\ OH^- \Rightarrow H_2O + 1/2\ O_2 + 2\ e^- \quad (4)$$

producing nearly pure oxygen (water saturated, but free of nitrogen, argon, and carbon dioxide). The minimum voltage, from equation (2), is but a few tens of millivolts.

The propensity for this alkaline electrolyte to scrub carbon dioxide from the air led to its application as a life-support subsystem in manned spacecraft[2]. When the electrolyte reaches a steady-state composition it is an alkaline carbonate solution, with a pH near 12 at the cathode and, with hydrogen supplied to the anode in place of electric power, a pH near 7 at the anode.

The same principle can be, and has been, applied to high temperature gas mixtures encountered in coal utilization. These are the two general types of processes: reducing, as from gasification processes; and oxidizing, as in combustion flue gas. The primary gaseous pollutant in each case is a sulfur species; in the first case H_2S and in the second case SO_2. Since the membrane is exposed to the same pressure on both sides, there is no theoretical limit to the pressure at which the process operates. While the electrochemical principle is the same for each, the chemistry is quite different; the main thrust of this research is the purification of fuel gases (specifically coal gasification product gases, or synthetic-gas) of H_2S.

Four major task were designated, as stated in the proposal for H_2S & SO_2 removal:

H_2S

1. Find a suitable anode material capable of high current density while maintaining structural and chemical stability in the harsh cell environment.

2. Optimize and utilize membrane matrix materials sustaining morphology and providing a barrier to process gas-crossover in full-cell experiments.

SO_2

3. Manufacture of a suitable matrix by tape-casting, sintering, or pressing.

4. Determine viability of components in full-cell tests designed to achieve 90% removal.

H_2S SUMMARY

The gas resulting from coal gasification has a broad range of compositions depending on the coal as well as the gasification process; that is, the temperature, pressure, and amount of air (or oxygen) and steam employed. However, the level of H_2S is set by the sulfur content in the coal; for example, 3% sulfur coal will yield about 0.6 - 0.7% H_2S. A lesser amount of COS is found as well. The corrosive and toxic nature of these contaminants make it essential that they be removed down to sub-ppm levels.

Since gasification processes are quite varied, the product gas also has a large variety of compositions:

CO	18. - 60. %
CO_2	3. - 30. %
H_2	15. - 60. %
N_2	1. - 60. %
H_2O	2. - 30. %
H_2S	0.2 - 1.5%

Processes to remove the H_2S generally rely on low to ambient temperature absorption, followed by sorbent regeneration and Claus treatment for conversion of concentrated H_2S to elemental sulfur. Hot gas desulfurization has been limited to employment of metal oxide sorbents which suffer most of the same drawbacks as the lower temperature processes. That is, they require desorption and Claus treatment.

The hot-gas electrochemical membrane process is illustrated schematically in Figure 1. The product gas, cleansed of particulates, is passed by the cathode. Here, the most easily reduced component, that is, the strongest Lewis acid, will be electronated.

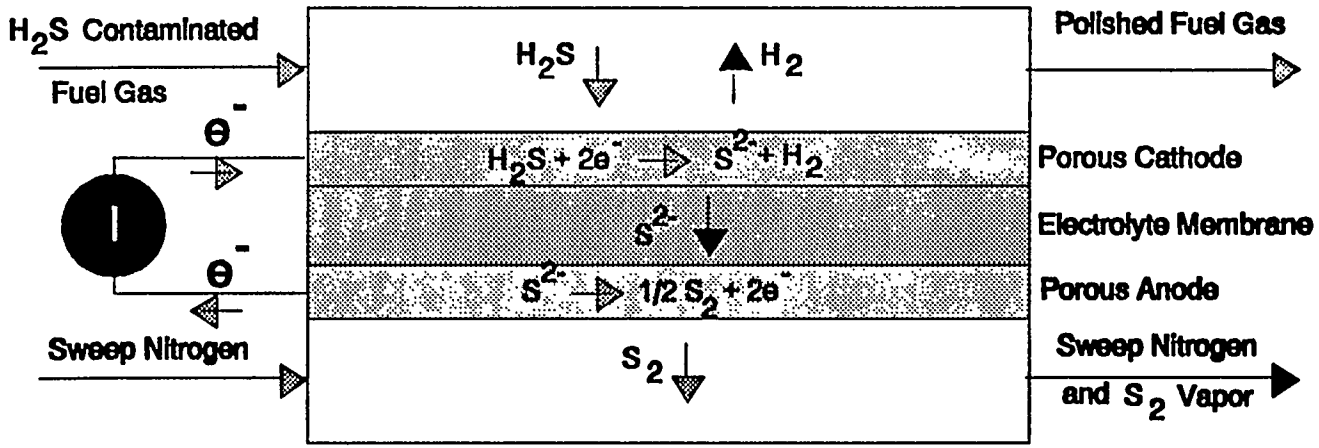

Figure 1 Electrochemical Membrane Separation Process

Under these conditions, it is H_2S:

$$H_2S + 2\,e^- \Rightarrow H_2 + S^{2-} \qquad (5)$$

A membrane which contains sulfide ions in a molten state will act to transport sulfide across to the anode where, in the simplest case, hydrogen can be supplied to form H_2S. If the membrane is capable of preventing diffusion of hydrogen from the cathode side, an inert sweep gas such as N_2 can be used at the anode to carry away oxidized sulfide ions as vaporous sulfur, S_2.

This concept has been used with success for gases containing only H_2S in N_2[3], simulated coal gases[4], and simulated natural gases[5]. For this last work, a membrane was constructed of alkali metal sulfides and carbonates retained in a porous MgO stucture a few millimeters in thickness. The cathode was made of porous carbon and the anode of porous CoS_2. Polishing of simulated coal gases, testing the most stringent application of this technology, has recently been shown using the electrochemical membrane separator. Successful polishing experiments utilized a porous cubic zirconia membrane of the same order thickness as previous membrane materials. Electrodes were lithiated-NiO. The cell is shown schematically in Figure 2. As anticipated, applied current acted to remove H_2S from the cathode gas, as shown in Figure 35 & 36. It was simultaneously produced at the anode:

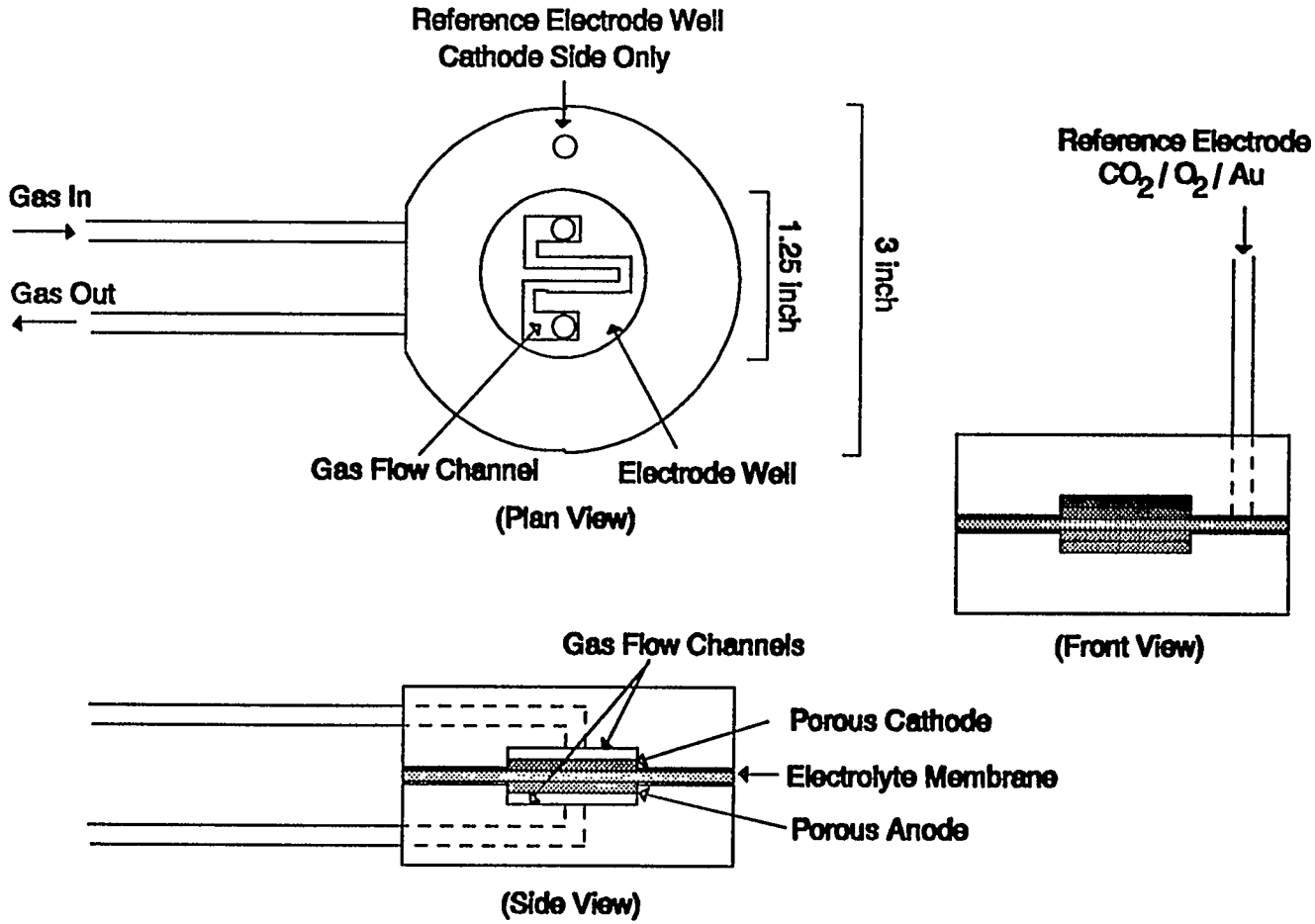

Figure 2 Schematic of Electrochemical Cell

$$S^{2-} \Rightarrow 1/2\ S_2 + 2\ e^- \quad (6)$$

The situation is complicated, however when realistic gas mixtures are involved. Carbon dioxide and water vapor compete in the reduction reaction by:

$$CO_2 + H_2O + 2\ e^- \Rightarrow CO_3^{2-} + H_2 \quad (7)$$

As reaction (7) proceeds at about the same standard potential as reaction (5), the electrolyte becomes richer in carbonate. The ionic flux through the membrane depends upon the relative mobilities of the carbonate and sulfide as well as their concentrations.

Since the oxidation reactions (6) and (8):

$$CO_3^{2-} + H_2 \Rightarrow CO_2 + H_2O + 2\ e^- \quad (8)$$

also occur near the same standard potential, about 1 Volt positive of the reductions, CO_2 will be transferred at a far greater rate than H_2S, since it will be present in the process gas at an order of magnitude higher concentration.

$$E = E^\circ - [RT/nF] \ln(a_{prod.} / a_{react.}) \quad (9)$$

The situation is favorably altered if no reductant is available at the anode. The direct oxidation of carbonate:

$$CO_3^{2-} \Rightarrow CO_2 + 1/2\ O_2 + 2\ e^- \quad (10)$$

occurs at a standard potential some 700 mV more positive than that for sulfide:

$$S^{2-} \Rightarrow 1/2\ S_2 + 2\ e^- \quad (6)$$

Thus, a concentration (or activity) ratio of 10^5 could exist in the anolyte, assuming equivalent electrode kinetics for the two reactions, before significant (e.g. 1%) carbonate is oxidized. This mode of operation is preferable for commercial application, with direct

production of elemental sulfur vapor, eliminating the need for a Claus reactor. The net effect, under these conditions, is continuous removal of H_2S from the process gas accompanied by enrichment of the process gas with H_2 and direct generation of elemental sulfur. The only reagent required is electric power at a potentially attractive rate.

The equilibrium potential for a single cell, given by equation (9), for the cathodic and anodic reactions (5) and (6), is 587 mV for a process gas containing 100 ppm H_2S and an anode product of pure sulfur vapor. To this must be added the overpotentials needed for both electrode reactions and ohmic loss. The electrode reactions have been studied in free electrolyte on graphite electrodes[6,7]. Potential step experiments showed very rapid kinetics, with exchange currents in both cathodic and anodic directions near 40 mA/cm^2. Cyclic voltammetry verified a 'catalytic' reaction mechanism with disulfide as the electro-active species. At the cathode:

$$H_2S + S^{2-} \Rightarrow H_2 + S_2^{2-} \quad (11)$$

and

$$S_2^{2-} + 2\,e^- \Rightarrow 2\,S^{2-} \quad (12)$$

At the anode:

$$S_2 + 2\,S^{2-} \Rightarrow 2\,S_2^{2-} \quad (13)$$

$$S_2^{2-} \Rightarrow S_2 + 2\,e^- \quad (14)$$

Surprisingly, enhanced cathodic H_2S removal was found with CO_2 and H_2O in the gas, probably due to another 'catalytic' scheme, reaction (7) followed by:

$$CO_3^{2-} + H_2S \Rightarrow CO_2 + H_2O + S^{2-} \quad (15)$$

Another unexpected result was the concurrent removal of the COS down to levels below the analytical limit (ca. 1 ppm). This occurs apparently due to rapid equilibrium between H_2S, CO, CO_2, and COS at these temperatures.

A study of potential cathode materials[4] showed several promising alternatives. It was conducted using a configuration similar to anticipated designs (see Figure 2). Since the working membrane will be mostly carbonate at steady-state, Molten Carbonate Fuel Cell(MCFC) 'tiles', purchased from IGT, were used. Other membrane materials such as a tape cast MgO, zirconia felt, and rigid zirconia each infiltrated with molten carbonate in the same cationic mole composition($Li_{0.62}K_{0.38}$) used in the MCFC, sulfided in-situ, provided sufficient barriers to process gases and electrolyte entrainment to attain high removal of H_2S (over 90%). Several electrode materials were found acceptable; including nickel and cobalt, formed from powders, sulfided in-situ.

Studies of 'tile' compositions have also been performed. By analyzing the equilibrium of reaction (16), it is possible to know the electrolyte composition which would be in equilibrium with a given process gas at a given process temperature. This has been done with some success by Alexander (see Figure 3)[5]. Theoretical tile compositions were calculated by thermodynamic analysis of the tile equilibrium reaction (16). Since standard MCFC tiles were used in this analysis, the cations present were K and Li in a ratio corresponding to the low melting carbonate eutectic ($Li_{0.62}K_{0.38}$).

$$(Li_{0.62}K_{0.38})_2CO_3 + H_2S \;<=>\; (Li_{0.62}K_{0.38})_2S + CO_2 + H_2O \qquad (16)$$

This analysis was performed by finding the Gibbs free energy of reaction (16) at the process temperature and relating this to the equilibrium constant, K_a, by the relation:

$$\ln K_a = \frac{\Delta G}{RT} \qquad (17)$$

with K_a defined as:

By this analysis, a process gas with a composition of 0.88% CO_2, 1760 ppm H_2S, 12% H_2O, and the balance methane (for the natural gas process mentioned above) with a run

$$K_a = \frac{P_{CO_2} P_{H_2O} a_{(Li_{0.62}K_{0.38})_2S}}{P_{H_2S} a_{(Li_{0.62}K_{0.38})_2CO_3}} \qquad (18)$$

temperature of 610° C will have an equilibrium constant of 6.9. If the activity coefficients of the molten phase constituents (namely the sulfide and carbonate in the electrolyte) are assumed to be unity, this translates to an electrolyte composition of 19.5% sulfide and 80.5% carbonate. This was verified by exposing a tile which was originally 100% carbonate to the above process gas for 34 hours in an operating removal cell. The tile was subsequently analyzed by wet test methods and found to have a composition of 20.3% sulfide and 79.7% carbonate.

If a 'tile' is manufactured already in equilibrium with the gas to be treated, it will not have to undergo the stresses inherent in the density changes associated with 'sulfiding' a carbonate tile or 'carbonating' a sulfide tile. While techniques for manufacturing such a tile are still under study, the concept has been used successfully in both the coal gasification process cell[8] and the natural gas process cell[5].

The key to successful anode performance; that is, oxidation of sulfide but not carbonate, will depend upon identifying an anode material capable of overpotentials below about 500 mV at current densities of 100 mA/cm^2. This would seem possible

since it has been achieved with graphite and since cathodes have been operated at relatively high current densities well within this limit. Several potential anode materials have been identified[8] and anodes of CoS_2 have been used with some success in the natural gas process cell[5]. Anodes constructed of these materials do not have the chemical decomposition problems inherent in the carbon electrodes. NiO used primarily in molten carbonate fuel cells have also shown promise in full-cell experimentation as an adequate anode material.

MATERIALS

Electrodes

The electrodes used as sites for the electrochemical reduction and oxidation reactions in this removal cell must meet certain criteria with respect to their materials and their pore characteristics. They must be electronically conductive within the temperature range of operation for the cell and they must be chemically stable in the corrosive process gas and the oxidizing environment of the anode. The pores through the electrode must offer little gas phase diffusion resistance since reagents must be able to move from the bulk gas phase to the reaction sites at the electrode/electrolyte interface. The overall pore structure must have a high interfacial surface area in order to maximize the sites for electrochemical reaction. Finally, the electrode pores must offer low capillary forces on the electrolyte within the membrane matrix. The electrolyte must only wet the walls of the electrode pores, not completely flood the electrode. If the

electrode floods, the interfacial surface area is decreased and the membrane matrix is depleted of electrolyte.

Several potential electrode materials were identified by Weaver[8]; of these, porous carbon, $La_{0.8}Sr_{0.2}CrO_3$, Co, CoS_2, MoS_2, Ni and NiO were used in full-cell experiments. Since Weaver has surveyed possible cathode materials, interest in this study was placed on possible anode materials tested in a removal cell with a gas-impermeable membrane.

Carbon: Carbon is highly conductive and remains solid to an extremely high temperature. Electrodes were obtained from Ultra Carbon pre-formed with dimensions of 1.25" diameter and 0.8 mm thick (porosity of 54%). While useful for short duration bench-scale experimental runs, carbon would not be useful in an long duration or industrial application because of degradation reactions. At the cathode it is eroded by steam or CO_2:

$$C + H_2O \rightarrow CO + H_2 \qquad (19)$$

$$C + CO_2 \rightarrow 2\,CO \qquad (20)$$

And at the anode it can act as a reductant for carbonate:

$$CO_3^{2-} + C \rightarrow CO + CO_2 + 2e^- \qquad (21)$$

Since reaction **(21)** occurs at a potential about 300 mV below the sulfide oxidation reaction, this provides a 'short-cut' for carbonate transport. Thus, carbon was not useful

as an anode material. However, since carbon electrodes were inexpensive and easily available, they were used as cathode materials in experimental runs of limited duration, specifically in natural gas application studies. Carbon cathodes were used successfully in runs 37, 40, and 42.

Carbon anodes act as a reducant for CO_3^{2-} by (21); therefore, carbon was not the material of choice for use as the anode. Carbon anodes showed sever degradation over the course of relatively short runs (around 48 hours). Since they were easily available some runs did use carbon anodes with limited success.

$La_{0.8}Sr_{0.2}CrO_3$: The high melting temperature, corrosion resistance, and high electrical conductivity of certain ceramic materials identify them as possible candidates for removal cell electrodes. Lanthanum chromite, $LaCrO_3$, is a p-type semiconductor due to holes in the conduction band of Cr^{3+} ions[9]. Doping either La^{3+} or Cr^{3+} sites with a lower valence ion, in this case Sr^{2+}, results in enhanced conductivity due to formation of Cr^{4+}. The position on which the electron acceptor dopant ion substitutes is determined by its ionic radius according to Pauling's rules[10].

$La_{0.8}Sr_{0.2}CrO_3$ semiconducting metal oxide was purchased as a powder from HUA Associates of Rolla, MO. This material was prepared using a gel-precipitation technique which produces finely dispersed particles of homogeneous composition. The 'as received' powders were screened to +100, 100-200,200-325, 325-400, and -425 mesh portions. Electrodes used for cell tests were prepared from 100-200 mesh powders by dry-pressing in a 1 1/4" die at 8000 psi. The resulting oxide discs were very fragile, thus

a sintering step was necessary to provide enough strength for use in the cell. By trial and error, sintering conditions were found to be 2 hours at 1350°C. This produced a structure with a bulk porosity of approximately 60% and a pore size of about 30 μm.

When used as a cathode material excellent physical and chemical stability was shown, but high ohmic losses through the electrode present inherent system problems. An anode was manufactured from this material and successfully used in the natural gas sweetening application. The electrode polarization, however, was found to be unacceptably high.

Metal Electrodes: Phase diagrams may be constructed for metal-sulfur-oxygen systems based on analysis of the Gibb's free energy of all stable phases within the system at a given temperature[11]. From these diagrams, the phase in thermodynamic equilibrium with the process gas stream can be determined.

For metal-sulfur-oxygen systems at 650°C, the stable phases will consist of metal, metal sulfide, metal oxide, and metal sulfate components. Weaver performed this analysis for Co, Mo, and Ni[12]. In his analysis, the gas phase activities were assumed to be equal to the partial pressure and solid phase activity was set equal to unity. The chemical reactions between the system compounds were written in terms of S_2 and O_2 activity.

The S_2 and O_2 partial pressures were related to actual stream components using the following equilibrium expressions:

$$H_2 + \frac{1}{2}O_2 \rightleftharpoons H_2O \qquad (22)$$

$$CO + \frac{1}{2}O_2 \rightleftharpoons CO_2 \qquad (23)$$

$$H_2 + \frac{1}{2}S_2 \rightleftharpoons H_2S \qquad (24)$$

All thermodynamic data was taken from Barin and Knacke[13, 14].

While useful in predicting "zero-current" thermodynamic equilibrium phases for metal-sulfur-oxygen systems, the phase diagrams generated by Weaver do not provide a complete picture of the system equilibrium because chemical kinetics, the effects of applied current (and induced potential), and reactions with the electrolyte species were not considered.

Preto has studied Ni-S and Co-S systems in molten LiCl/KCl electrolytes for use in Li-Al/FeS battery cells[15]. He showed that Ni and Co undergo simple oxidation/reduction transitions of the form:

$$M + 2S^{2-} \rightleftharpoons MS + S^{2-} \rightleftharpoons MS_2 \qquad (25)$$

Ingram has studied the oxidation of Ni to NiO within the molten carbonate fuel cell system[16]. He shows oxidation/reduction transitions of the form:

$$M + CO_3^{2-} \rightleftharpoons MO + CO_2 + 2e^- \qquad (26)$$

The potentials at which these reactions occur at 650°C were calculated from published data[13,14] and are presented in Table I.

Co, Co_9S_8, and CoS_2: Cobalt electrodes were converted to the stable metal sulfide phase in situ, similar to the technique used to produce the NiO cathode in a molten carbonate fuel cell. Metal powders (less than 2μm particle size) were purchased from Aldrich Chemical. The cobalt powder was evenly loaded into a 1 1/4" stainless steel die and dry pressed at 8000 psi total static pressure using a hydraulic ram. No sintering step was used in preparation of the metal electrodes due to the oxidation, cracking, and warping which occurred when the metal discs were heated in air.

High purity CoS_2 (particle size average of 75μm) was obtained from Alfa Chemicals and mixed with hydroxyethyl cellulose (HEC) from Union Carbide Corp. Void percentages as high as 60% were obtained using a mixture of 10 weight % HEC and 90 weight % metal-sulfide powder. This mixture was loaded into a 1 1/4" stainless steel die and pressed at 8000 psi using a hydraulic ram. The resulting electrode wafer was then heated at 350°C for 30 minutes to burn out the HEC. This final electrode was then cooled, weighed, and stored for use in the electrochemical cell.

Weaver reported Co-S electrodes as successful cathode materials. He reported Co_9S_8 as the stable phase under coal gas applications and showed by cyclic voltammetry that this compound was electrochemically reduced to Co metal and sulfide ion, providing a catal ::c mechanism for H_2S removal by:

$$Co_9S_8 + 16e^- \rightarrow 9Co + 8S^{2-} \qquad (27)$$

followed by:

$$9\,Co + 8\,H_2S \rightarrow Co_9S_8 + 16\,H_2 \qquad (28)$$

Cobalt cathodes used in several coal gasification experiments provided stoichiomatric carbonate transport across the cell, however removal of H_2S using cobalt metal is still under investigation.

CoS_2 was the material of choice for the anode in natural gas sweetening applications. This material showed excellent stability in the oxidizing enviroment of the cell, as long as the operating current of the cell did not run the anodic overpotential high enough to promote significant oxidation of carbonate. If the anode potenital was run too high during the course of the run, the material would oxidize, loose conductivity, and break-down as an electrode material. CoS_2 was used successfully in runs 37 and 38.

Table I Estimated Phase Transitions - Metal-S-O Systems at 650°C.

Phase Transitions for the Ni-S-O System

Transition Reaction (Oxidation)	Calculated Potential,V
$3Ni + 2S^{2-} \Rightarrow Ni_3S_2 + 4e^-$	0.922
$Ni_3S_2 + S^{2-} \Rightarrow 3NiS + 2e^-$	0.716
$Ni + CO_3^{2-} \Rightarrow NiO + CO_2 + 2e^-$	1.013

Phase Transitions for the Co-S-O System

Transition Reaction (Oxidation)	Calculated Potential,V
$9Co + 8S^{2-} \Rightarrow Co_9S_8 + 16e^-$	-0.018
$Co_9S_8 + 10S^{2-} \Rightarrow 9CoS_2 + 20e^-$	1.189
$Co + CO_3^{2-} \Rightarrow CoO + CO_2 + 2e^-$	1.067
$CoO + CO_3^{2-} \Rightarrow Co_3O_4 + CO_2 + 2e^-$	0.359

Ni and NiO: Ni electrodes were donated to this research by ERC as 8" by 11" sheets (pore size was proprietary, but average porosity was between 75 and 80%). A die was used to cut 1 1/4" electrodes from this sheet. These electrodes were then soaked in 1 M LiOH and then dried. If Ni electrodes were to be used, the electrodes were then loaded into the cell and the run was started. If NiO electrodes were to be used, the electrodes were placed between two sintered Al_2O_3 disks and placed in an oven at 650°C under atmospheric air for at least six hours. Gravimetric analysis of these oxidized electrodes showed that the Ni was at least 96% converted to NiO. This material was successfully used as the starting material for a cathode in run 43 of the natural gas polishing application and runs 47, 48, and 49 of the coal gas polishing application. Lithiated NiO was successfully used as the starting material for the anode in runs 42 and 43 of the natural gas polishing application and runs 47, 48, and 49 of the coal gas polishing application. Lithiated Ni was successfully used as the starting material for a cathode material in run 39 for natural gas polishing application and runs 55, 56, 57, 58, 59, 62, 65, 4, and 5 for coal gas polishing applications. Lithiated Ni was successfully used as the starting material for an anode in runs 39 and 40 for natural gas polishing application and in runs 55, 56, 57, 58, 59, 62, 65, 4, and 5 for coal gas polishing application.

X-ray diffraction of used electrodes from the natural gas polishing studies showed that the equilibrium structures were a mixture of several compounds, primarily Ni and NiO with traces of Ni_3S_2 and NiS present in both the cathode and the anode materials.

The x-ray diffraction scan of the cathode material used in run 39 showed that the equilibrium material was a mixture that was predominantly NiO, with smaller ammounts of Ni, Ni_3S_2, and NiS. The anode material in run 39 was shown to be entirely NiO. The anode material for run 40 was shown to be a mixture of Ni, NiO, and Ni_3S_2. The difference between run 39 and run 40 with respect to the anode was that run 39 removed CO_2 through the carbonate transport reaction:

$$CO_3^{2-} \rightarrow CO_2 + \frac{1}{2}O_2 + 2e^- \qquad (10)$$

O_2 from this reaction would have served to oxidize the initially Ni anode into NiO. In run 40, however, selective removal of H_2S was observed. NiO was present in the anode of run 40 to a lesser extent than run 39, and the presence of Ni_3S_2 is due to transported sulfide/sulfur.

The electrodes used in run 43 started as lithiated NiO. After 222 hours of operation, the cathode was shown to be a mixture of Ni, NiO, and Ni_3S_2, supporting the results obtained in run 39 even though the starting material was NiO rather than Ni. The anode of run 43 started out as pure NiO and remained unchanged even after 222 hours of operation.

X-ray diffraction of the materials used in the coal gas polishing application also showed primarily Ni and NiO with traces of Ni_3S_2 in the electrode materials. Run 49 started with NiO as both the cathode and anode material. After 216 hours of operation, the cathode was entirely Ni. The anode was a mixture of Ni, NiO, and Ni_3S_2.

Further investigation revealed H_2S levels in the coal gasification stream above 100 ppm created a molten electrode material of form Ni_3S_2 . This caused the reaction sites for the reduction of H_2S to diminish completely nullifying the E.M.S. removal capabilities. Alternate cathode materials must be utilized with coal gas streams containing higher than 100 ppm H_2S. Cobalt is the predominent candidate due to previous success in full-cell experiments.

Anode materials which were stable in the oxidizing enviroment of the anode side of the process cell were developed and tested. Ni-O-S and Co-S anode materials allowed operation of the cell with suffi(+(% *25^I^\ nt flux to accomidate the required H_2S removal rates while allowing the cross-cell potenital to remain low enough so that CO_3^{2-} was not preferentially transported across the cell.

Various candidate electrode materials have been tested and compared on the basis of physical and chemical stability, electrical conductivity, and electrochemical performance in an operating cell.

Electrolyte

The composition of the electrolyte present in the membrane of the cell reaches an equilibrium sulfide level based on the following reaction:

$$(Li_{0.62}K_{0.38})_2CO_3 + H_2S <=> (Li_{0.62}K_{0.38})_2S + CO_2 + H_2O \qquad (16)$$

Theoretical compositions are calculated through an analysis of the Gibb's free energy of this reaction yielding the equilibrium constant by:

$$\ln K_a = - \Delta G/RT \qquad (17)$$

with K_a defined as:

$$K_a = P_{CO2}\, P_{H2O}\, a_{M2S} \,/\, P_{H2S}\, a_{M2CO3} \qquad (18)$$

If the activity coefficients of the molten phase constituents (namely the sulfide and carbonate in the electrolyte) are assumed to be unity, then equation (18) becomes:

$$K_a = P_{CO2}\, P_{H2O}\, X_{M2S} \,/\, P_{H2S}\, X_{M2CO3} \qquad (29)$$

with X_{M2S} and X_{M2CO3} defined as the mole fractions of sulfide and carbonate present in the melt such that:

$$X_{M2S} + X_{M2CO3} = 1 \qquad (30)$$

Actual compositions are measured by gravimetric analysis of total sulfur species present after oxidation with hydrogen peroxide. A sample of membrane material is weighed and then dissolved in water. The insoluble matrix materials are filtered and the filtrate is treated with excess hydrogen peroxide which oxidizes all sulfur species to sulfate. It is assumed that only sulfur in the form of sulfide is present in the membrane under run conditions. This solution is then acidified with hydrochloric acid to decompose the carbonate to carbon dioxide and water. The solution is boiled to de-gas the mixture and then barium chloride is added, causing the sulfate to precipitate as barium sulfate. The solution is then filtered, and the precipitate is rinsed, ignited, and weighed. The moles of barium sulfate precipitated is directly related to the moles of sulfide in the electrolyte.

Since the mass of the original sample is known, and the mass of the insolubles is known, then the mass of the soluble electrolyte present in the sample is known by difference. It is assumed that carbonate and sulfide species are the only components of

the electrolyte, thus, the moles of carbonate is related to the moles of sulfide by equation (30). The results of this analysis are presented in Figure 3 for runs 37 through 40. Examination of this data shows that the equilibrium composition of the electrolyte can be closely approximated by the above analysis. The method is subject to a degree of experimental error, and this is shown in the variations between the theoretical and actual results. Still, the method does confirm the assumption of unity activity coefficients of the sulfide and carbonate species in the electrolyte melt.

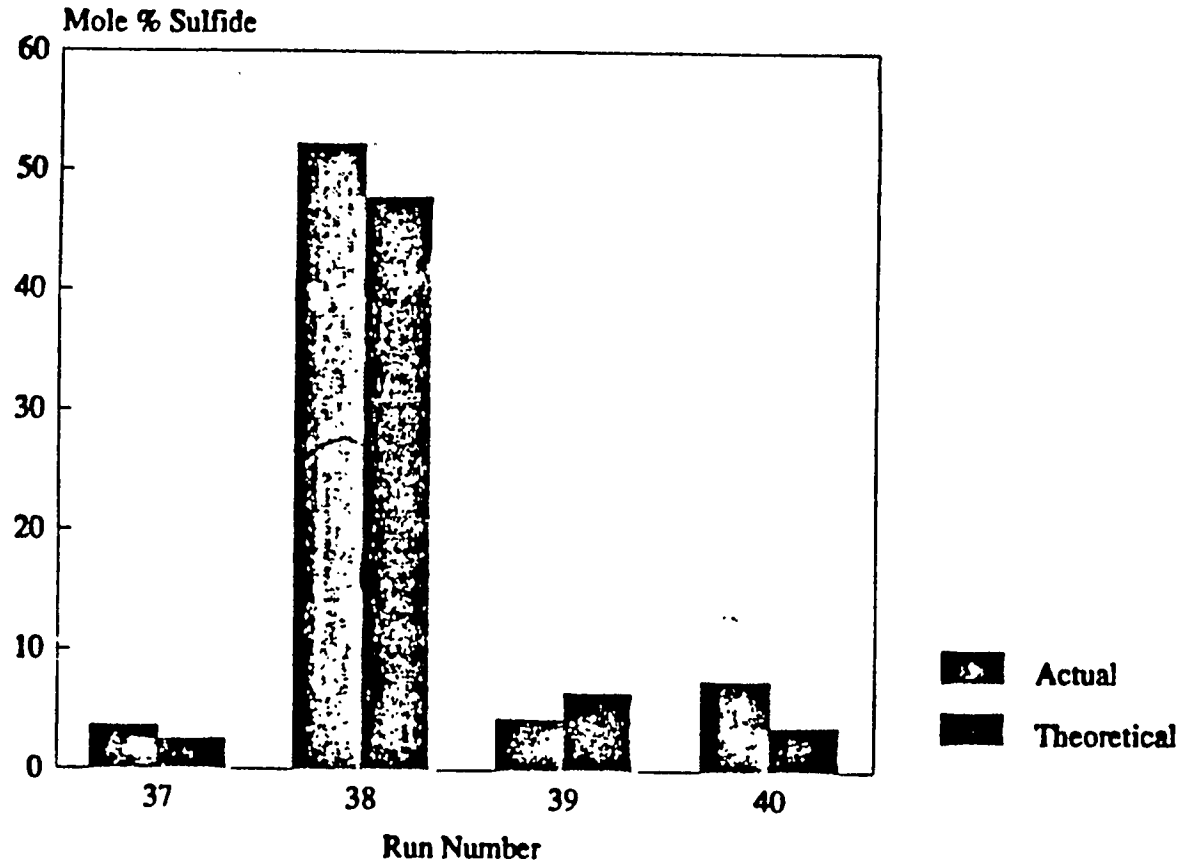

Figure 3 Electrolyte Composition (Actual vs Theorectical Sulfide)

Electrode Analysis: Electrode analysis consists of three phases: (1) solubles analysis, (2) insolubles analysis, and (3) bulk structure analysis. Each phase of the overall electrode analysis proceeds in the following manner.

Solubles Analysis

This phase proceeds in a manner very similar to the technique outlined above for membrane electrolyte analysis. First, the electrode sample is ground and weighed. It is then washed in a water bath where the soluble components are dissolved. The soluble components consist primarily of electrolyte salts which have wicked into the pores of the electrode structure. There may also be some soluble electrode materials in the form of metal sulfates. Dissolved metal sulfates can be tested for by atomic absorption, and access to this test method is currently being arranged. An attempt has also been made at determining the amount of dissolved metal sulfates by precipitation as metal hydroxides but the presence of barium and lithium in the final filtrate solution makes this method questionable as these metal hydroxide species are also insoluble. The results of this testing are discussed for certain experimental runs in the results section of this report.

Insolubles Analysis

This phase of electrode analysis is performed using x-ray diffraction. The results of this testing are discussed for certain experimental runs in the results section of this report.

Bulk Structure Analysis

This phase of electrode analysis is performed using scanning electron microscopy (SEM) techniques. The results of this testing are used intermitently to insure the integrity of materials for the E.M.S.; however, due to the quality of photo-copied S.E.M. pictures inclusion is not possible.

Matrix

Perhaps the most important issue facing the E.M.S. is finding an adequate membrane material. A suitable matrix material must meet three criteria (1) be chemically and electrically stable in the E.M.S. environment, (2) provide a consistent pathway for ionic transfer (small pores to maintain complete electrolyte flooding of the matrix material while wetting the electrode pores with electroyte), and (3) provide a barrier against process gas cross-over from the cathode side of the cell to the anode side in order to deter alternate reactions. Several materials have been invetsigated including MgO, $LiAlO_2$, and yttria-stabilized zirconia.

MCFC membranes: Early experiments used Molten Carbonate Fuel Cell(MCFC) membranes (eutectic Li/K carbonate electrolyte hot pressed within a $LiAlO_2$ matrix in approximately a 50/50 weight ratio) which were donated by GRI. These membranes were placed in the cell and allowed to go to their equilibrium sulfide levels in-situ. Successful H_2S removal has been recorded with the natural gas sweetening applications; therefore application in run 42 for natural gas experimentation utilized this membrane

successfully as shown in Figure 10. Also a GRI membrane with sufficient Li_2S sprinkled onto the membrane to bring it to its equilibrium sulfide level after the electrolyte had melted was successfully used with the coal gas polishing application in run 58, shown in Figure 22.

Density changes inherent with in-situ sulfiding of an initially carbonate electrolyte caused cracks within these membranes after a few hours of operation. The only exception to this was run 42. Since this was a natural gas polishing application, the equilibrium sulfide level was low enough that density change stress within the electrolyte did not appear to damage the membrane. Use of these membranes was discontinued in favor of manufacturing techniques which allowed customization of the electrolyte composition and improved matrix structure capable of handling more thermal and mechanical stress.

Hot Pressing: Several methods for the manufacture of the electrolyte membrane were developed and tested. Previously 'hot-pressing' was used in which powders of matrix material and electrolyte are intimately mixed in a dry atmosphere. They are then measured into a die and pressed into a tile at 5000 psi or greater pressure, 5°C or so below the electrolyte melting point. In the case of the sulfide/carbonate membranes, this temperture is determined from the phase diagram of Babcock[17]. This technique was used with success with application to the natural gas sweetening process. Since the membrane must be able to prevent bulk H_2 cross-over from the cathode to the anode side in order to selectively remove H_2S from the process gas, the technique was

abandoned since it was very difficult to manufacture a membrane without micro-cracks inherent in the structure. The technique involves two thermal cycles (heat-up to press the structure, cool down to release the structure, and heat-up within the cell housings), a sever mechanical shock (removing the heated piston from the die after pressing at elevated temperature), and a single handling step (cleaning the Graphite Foil, used as a die release material to prevent the membrane from bonding to the steel die, from the membrane surfaces) before the membrane can be used. Completely selective removal of H_2S from the process gas stream could not be achieved with this technique.

Sintered Ceramic Matrix: The second technique previously used involves the manufacture of a partially sintered ceramic matrix without electrolyte present and then wicking the molten electrolyte into the matrix voids by capillary action. This created a ceramic matrix with more structural integrity than the hot-pressed structures since the ceramic particles were actually bonded together to form a porous structure. The electrolyte flooded the pores and channels within this structure. This technique was used successfully with natural gas sweetening. Sulfur recovery in the anode sweep tubes was recorded in several experiments.

While the process selectivity was improved over the GRI membranes and the hot-pressed membranes, the membranes were still suseptable to thermal and mechanical stress during manufacture and cell operation. After the partially sintered body was formed, the membrane had to undergo thermal cycle as the electrolyte was melted into the structure and another as the cell was heated to its run temperature. The membrane

was mechanically stressed during handling between the processing steps. This membrane was also sensitive to density changes within the electrolyte. Equilibrium level sulfide electrolyte was wicked into the structures used in several runs under a N_2 blanket to relieve electrolyte density change stress on the membrane.

Zirconia Mats: The third technique recently used involved utilizing woven ZrO_2 textiles purchased from Zircar, Inc. These were pre-made woven ceramic fiber textiles made of Y_2O_3 stabilized ZrO_2. Woven cloth of 30 mil and 15 mil thickness was purchased and used as a matrix material by wicking molten electrolyte into the structure in-situ. This technique was used successfully with natural gas sweetening application and natural gas polishing application.

The average pore size of the zirconia textile structure has a bimodal distribution around 10 μm and 70 μm. While the structure had the ability to withstand thermal and mechanical stresses, the open aspect of the matrix (83% voids) allowed enough H_2 cross-over to keep selectivity low. The situation was improved somewhat when equilibrium level electrolyte was used or when the equilibrium sulfide level was low since the matrix did not have to contend with density stresses within the electrolyte. A denser structure was needed to hold the electrolyte and prevent gas cross-over.

Tape-casting: The fourth technique for membrane manufacture utilized tape-casting technology. By this method, the matrix material, dispersed along with an organic binder in a liquid, was formed into a dried tape along a glass substrate, maintained at

constant thickness by an overhead bird bar. The solvents from the slurry were then dried out and the ceramic/organic tape was the peeled off the surface of the substrate. The flexible 'green' tape was cut to the desired size and laminated under pressure with another flexible 'green' tape of ceramic material until the desired membrane thickness was achieved. The binders are then volatilized out in the process cell in an inert atmosphere or burned out of the cell under pure O_2 and the electrolyte was allowed to soak into the intersitial voids of the matrix powders, forming a membrane 'paste' between the gas diffusion electrodes.

The best results from tape casting were obtained using 'packaged' organic binder/solvent solutions purchased from Metoramics, Inc. By trial and error, the optimum ceramic/binder ratio for tape casting MgO within an their acrylic binder system K565-4 (the exact nature of the polymer is proprietory to Metoramics) was found to be 16.5 wt% MgO (Fisher, 325 mesh). This made a 'green' tape that was 44.4 wt% MgO (18.2 vol%) after solvent evaporation.

This technique for membrane manufacture was used successfully in run 43. Other unsuccessful experimental runs were attempted. After binder burn-out, the membrane was just a layer of powder with no structural integrety at all. The addition of electrolyte turned these powders into an electrolyte paste between the electrodes. As long as there was no gap between the electrode and the edge of the electrode well, tape casting worked well. However, the nature of the bench scale apparatus made it difficult to insure that there was no gaps anywhere around the circumference of the electrode (a perfect fit was required). In order to prevent the Ni/NiO electrodes from warping as

they went to their equilibrium structures, some gap between the electrode edge and the housing well was required. Tape cast membranes would fail at these gaps and allow bulk mixing of the process streams.

In answer to the need for a dense powder membrane with structural integrety, the fourth technique developed for membrane manufacture uses a composite structure in which a mat of woven yttria stabilized zirconia cloth with tape cast MgO 'bubble barriers' on each side of the membrane after the method of Iacovangelo and Karas[18]. The bubble pressure barrier concept provides a layered structure, with two tight matrix layeres on each side of a more open matrix layer. Any gas cross-over would have to find a single path through all three electrolyte filled matrix layers.

Using this concept, tape cast MgO was layered with zirconia cloth to operate successfully in runs 38 and 40 in the natural gas polishing application. Runs 49 and 57 successfully used this layered structure in coal gas polishing application of this technology.

Densified Zirconia: The fifth an final technique for membrane manufacture that was attempted came from the need to have an extremely dense ceramic membrane that still had enough structural integrety to withstand the thermal and mechanical stresses inherent in our experimental apparatus (an ultimately future industrial application). Zirconia cloth was densified with an inert ceramic powder (MgO, ZrO_2, or $LiAlO_2$) by suspending the powders in a slurry with ethanol and then soaking the mat in the slurry while pulling a vacuum on the vessel containing the mat and slurry. This vacuum de-

airs the voids of the mat and aids in the wetting of the woven material with the ceramic slurry. Zircar, Inc., had used similar techniques to create ceramic gas diaphrams with an average pore size of only 0.03 μm[19]. Such a structure would be dense enough to prevent the bulk diffusion of gases through the membrane and both strong and flexible enough to withstand localized density changes in the electrolyte due to carbonate/sulfide equilibrium shifts.

Membranes of this nature were used with success in run 59 (densified with 325 mesh $LiAlO_2$ from Aldrich), 60 (densified with sub-micron ZrO_2 from Zircar), 62 (densified with ZrO_2), and 65 (densifided with ZrO_2) in application of this technology to coal gas polishing.

FULL CELL TESTING

The following is a compilation of the most outstanding experiments done during the funding period. These are based on high removal of H_2S, low polarization, and low carbonate transport compared to sulfide transport. Other runs are entered to give a more detailed analysis of material issues and the thought process in determining the best possible E.M.S. set-up.

Run 38

This experimental run was the second polishing application run and used three mats of ZYW-30A zirconia cloth layered with three cast tapes of MgO ceramic as a membrane material. The MgO was present as a densifier for the membrane matrix to

prevent H_2 cross-over and subsequent transport of CO_2 across the cell. The electrolyte was lithium/potassium carbonate eutectic and was layered into the membrane during set-up. Both the cathode and the anode in this experiment were CoS_2.

A nitrogen sweep was applied to both sides of the cell and the cell was loaded into the furnace for heat-up. The binder from the MgO tapes was volatilized out at 375°C overnight. The pressure on the pneumatic ram was only 2.5 psi during volatilization and was increased to 5 psi once run temperature was reached.

Examination of the data presented in Figure 4 shows that the densification of the matrix appears to have worked. Completely selective removal of H_2S from the process gas was achieved. The overpotential data presented in Figure 5 shows that the 1 volt cross-cell potential threshold was never crossed during the period of time that this data was taken. No elemental sulfur was collected; since the concentration of H_2S was so low, a negligible amount of sulfur would have been produced. The cell ran for 130 hours and was shut down due to break-down of the anode, probably due to the slow oxidation of CoS_2 at higher potentials. With transport of CO_2 at higher potentials, O_2 would also have been produced, reacting with the CoS_2 to form cobalt oxide species and sulfur dioxide. Since cobalt oxide is not conductive, this would have driven the anodic overpotential higher and thus made the situation worse, increasing the rate of cobalt oxidation. This situation was observed, with rapid decay of the cobalt disulfide anode once CO_2 transport started and a possible sulfur dioxide peak appearing in the anode sweep gas chromatograph (the signal was retained too long in the column to have been H_2S or COS).

An analysis of the membrane electrolyte from this run showed a sulfide level of 52.2 mole% and a carbonate level of 47.8 mole% (see Figure 3) with 58.2 wt% insolubles. This compares with theoretical values of 45.7 mole% sulfide and 54.3 mole% carbonate (in equilibrium with 0.963% CO_2, 0.212% H_2S, and 3.2% H_2O). Dissolved $CoSO_4$ was subtracted from the total sulfur results by precipitating Co from the filtrate.

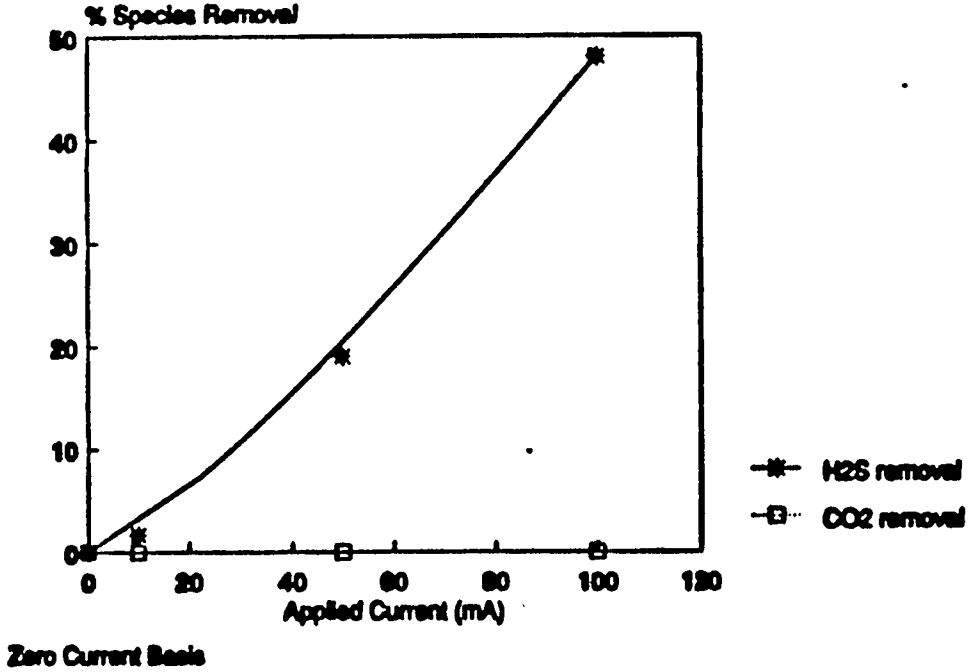

Figure 4 Run 38: Species Removal vs Applied Current

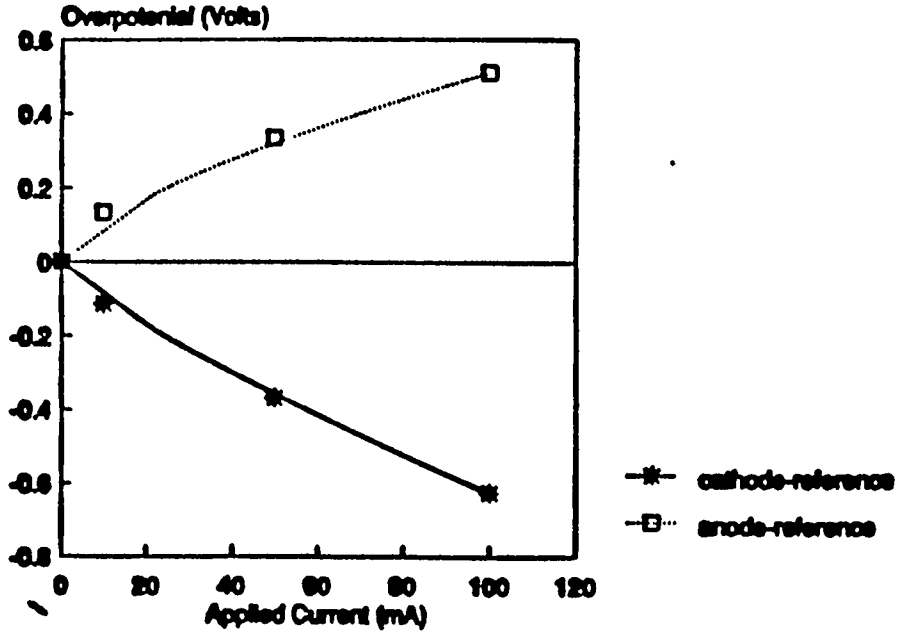

Figure 5 Run 38: Overpotential vs Applied Current

The composition of the Co precipitate from run 38 was verified by ashing to Co_2O_4. The Co precipitates (assumed to be $Co_2O_3*3H_2O$) were taken and ashed at a temperature of 850° C. This resulted in a black-purple substance with a recorded weight change which corresponded closely to the predicted change for $Co_2O_3*3H_2O$ going to Co_2O_4.

Run 40

This experimental run used a layered membrane structure similar to that used by run 38, except that the layers of ZYW-30A were contacting the wet seal areas instead of the cast MgO tape. Aluminum foil gaskets were also cut and laid into the wet seal area between the membrane and the MACOR housings. This was done in an attempt to improve the wet seal of the cell by intimately binding the membrane structure to the MACOR housings with a layer of $LiAlO_2$ formed in-situ. During heat-up to run temperature, the aluminum was converted to Al_2O_3 and then to $LiAlO_2$ through a subsequent reaction with Li_2CO_3:

$$Li_2CO_3 + Al_2O_3 <=> 2LiAlO_2 + CO_2 \qquad (31)$$

This run used carbon at the cathode and Ni (converted to NiO in-situ) at the anode. The choice of carbon was made in an attempt to isolate electrochemical H_2S removal by working around the "sulfide sink" presented by allowing an Ni electrode form metal sulfide species in-situ. The process gas for this run had a composition of 98 ppm H_2S, 1.45% CO_2, 3.9% H_2O, and balance CH_4.

Initially, cell seals were excellent. No cell cross-flow was detected and the cell was capable of pushing several inches of water back pressure. However, approximately 23 hours into the run a malfunction in the temperature controller allowed the cell to cool off to room temperature. N_2 was started to both cathode and anode sides of the cell as soon as the fault was detected and the controller was repaired. Unfortunately, the membrane was slightly damaged during the cool-down from run temperature. The $LiAlO_2$ gaskets lost integrity and began to leak. Cathode side to anode side bulk cross-flow was also detected. Current collector / electrode / membrane contact was also damaged as cross-cell resistances went from 0.9Ω to 4.0Ω. The cell would still pass current however, and cross-flow could be limited to cathode to anode side flow by decreasing the anode sweep flow rate. H_2S levels in the process gas were brought as low as 2 ppm (below GC analytical limits) (see Figure 6) over the course of the run with application of as little as 5 mA (cathode flow rate = 450 cc/min) with cross-cell potentials of only around 0.8 volts (see Figure 7) and no detectable CO_2 removal.

After 135 hours of operation, the cell was shut down for post-mortem analysis. The carbon cathode, while still operational, had degraded and was showing obvious signs of H_2O vapor erosion. The current collector on the anode side had also dissolved which explained the poor performance of the anode late in the run. A yellow tint was observed covering an area on the anode side wet seal were the seal had failed and was allowing sweep gas to be blown into the furnace.

Post-mortem analysis of the membrane showed an actual sulfide level of 7.5 mole% and a carbonate level of 92.3 mole% with 60.1 wt% insolubles present.

Theoretical analysis predicted a sulfide level of 3.7 mole% and a carbonate level of 96.3 mole%(see Figure 3).

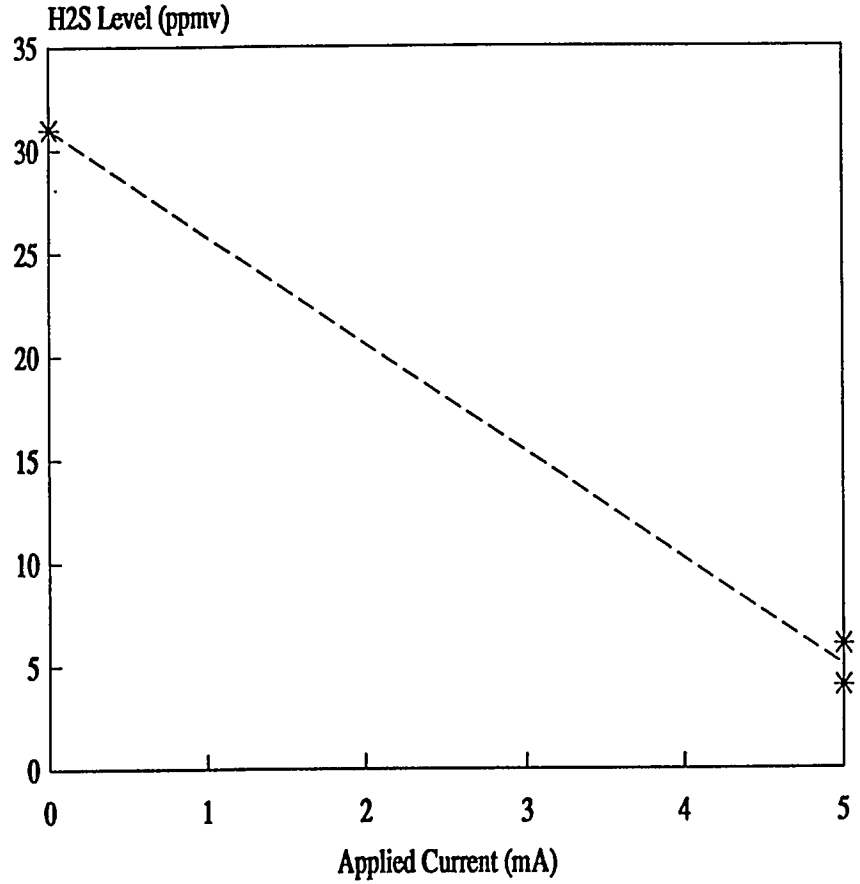

Inlet: 98 ppmv H2S
Cathode Flow = 225 cc/min

Figure 6 Run 40: Species Removal vs Applied Current

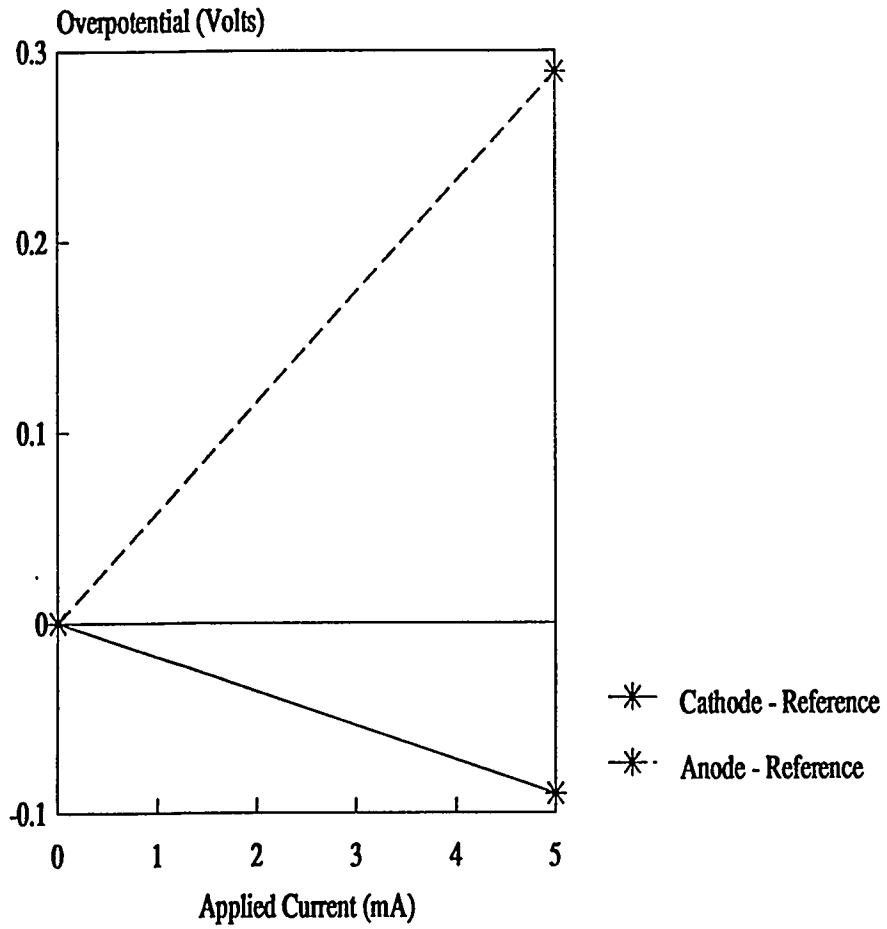

Figure 7 Run 40: Overpotential vs Applied Current

An analysis of the anode showed that the structure was only 62.9% flooded. The electrolyte which was wetting the pores of the electrode had an approximate composition of 4.8 mole% sulfide and 95.2 mole% carbonate. An analysis for dissolved $NiSO_4$ was not performed. Examination of the x-ray data presented in Figure 8 shows that the primary insoluble species are Ni and NiO, as expected in this run environment. However, when the scale is decreased as in Figure 9, Ni_3S_2 is seen to be present.

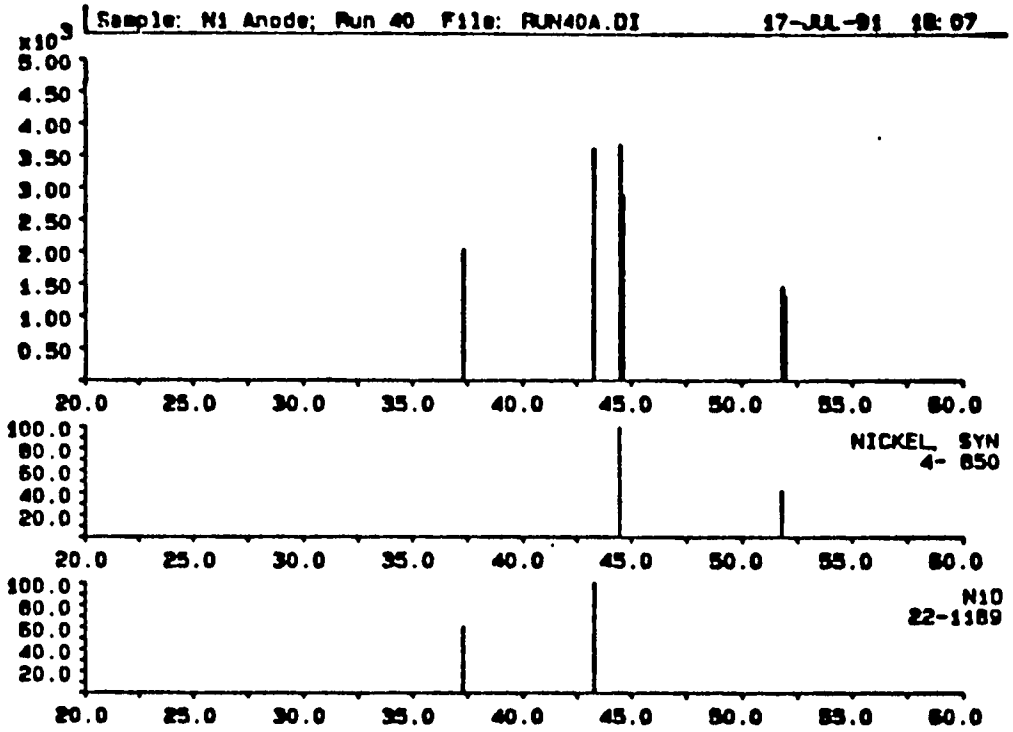

Figure 8 Run 40: Anode X-Ray Diffraction Pattern

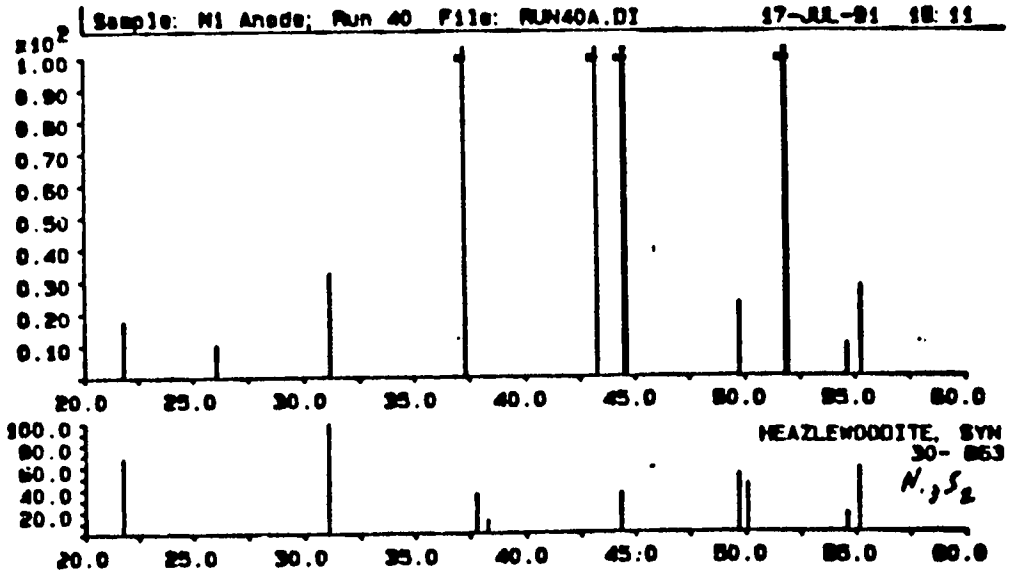

Figure 9 Run 40: Anode X-Ray Diffraction Patterns (Detail)

Run 42

This attempt at using MCFC tiles as membrane materials was more successful. Once again, the tile had $LiAlO_2$ as the matrix material with eutectic composition Li_2CO_3 and K_2CO_3 as the electrolyte. The cathode was carbon and the anode was lithiated NiO. Carbon was used as the cathode material in an atempt to eliminate the sulfide capacitance effects as Ni is converted to NiS or Ni_3S_2 (as in Run 40). The NiO anode was manufactured by soaking Ni electrode material from ERC in 1M LiOH and then heating to 650°C overnight. Weight analysis of the resulting electrode showed greater than 98% conversion of Ni to NiO. The process gas for this run, a simulated natural gas, had a composition of 1.44% CO_2, 97 ppm H_2S, 4.4% H_2O, and the balance CH_4.

Completely selective removals of H_2S as high as 98% (97 ppm down to less than 2 ppm) were observed with negligible cross-cell potential and 2.5 mA applied to the cell (0.32 mA/cm^2) at a process flow rate of 200 cc/min. This corresponds to 98% current efficiency. At higher process flow rates 75.2% removal of H_2S (97 ppm down to 24 ppm) with 5 mA applied to the cell (current density of .64 mA/cm^2) and a process flow rate of 450 cc/min was observed. This current density should have given 88% removal. This corresponds to a current efficiency of 85%. Figure 10 shows the H_2S removal vs applied current.

An analysis of the electrolyte from this run showed the sulfide level at 6.7% and the carbonate level at 93.3%. This corresponds to predicted values of 2.8% sulfide and 97.2% carbonate. This discrepancy between the predicted values and the actual values can be explained by the presence of an unknown slag found in the crucible after ashing

to recover the $BaSO_4$; the $BaSO_4$ precipitate was not adequately washed during the filtering process. X-ray analysis of the membrane material shows only $LiAlO_2$ and the hydrated forms $LiOH*2Al(OH)_3*xH_2O$ and $Li_2Al_2O_4*xH_2O$ present. Evidently, the low sulfide levels were not sufficient to cause attack of the $LiAlO_2$ matrix. The hydrated species of $LiAlO_2$ were no doubt formed when the membrane material was washed overnight in water to dissolve the electrolyte species out of the matrix. X-ray analysis results are presented graphically in Figure 11.

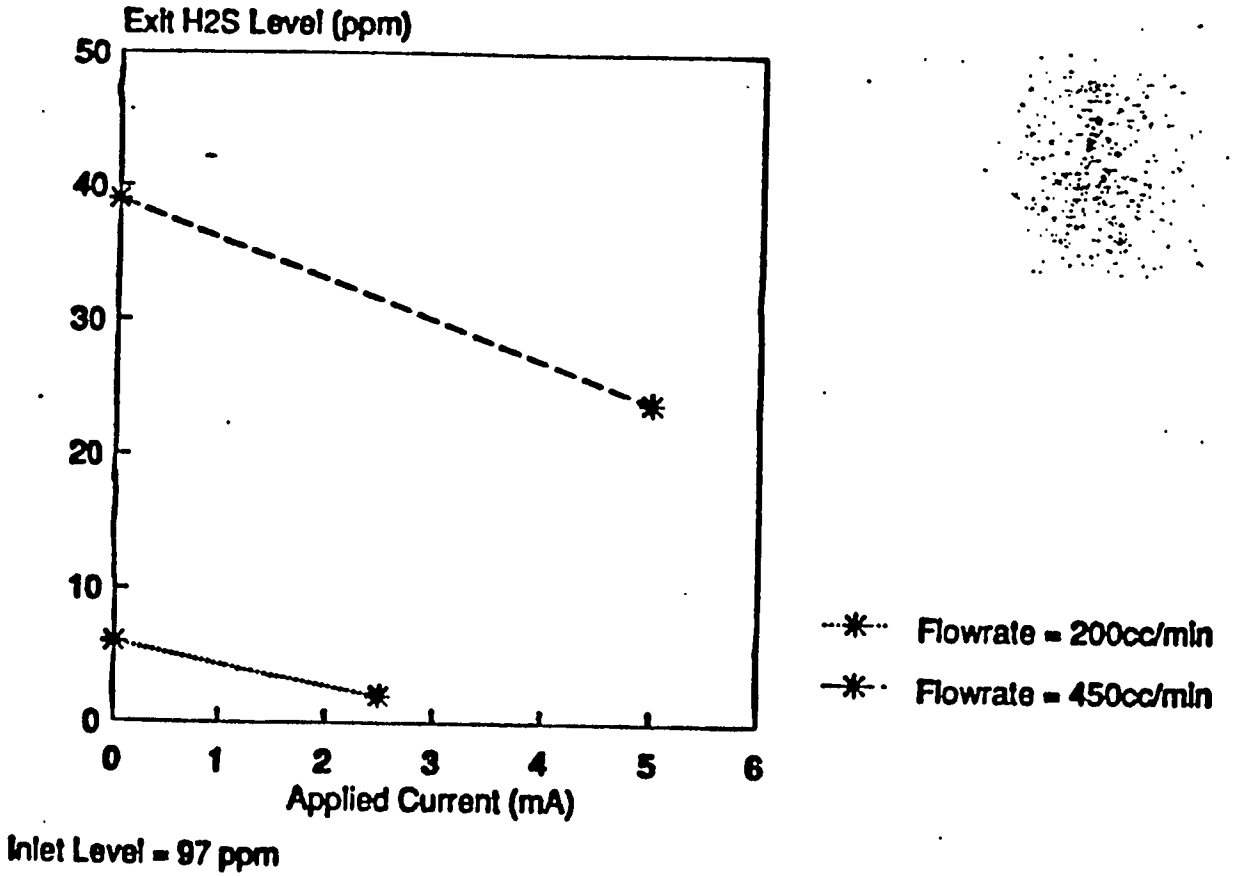

Figure 10 Run 42: H_2S Level vs Applied Current

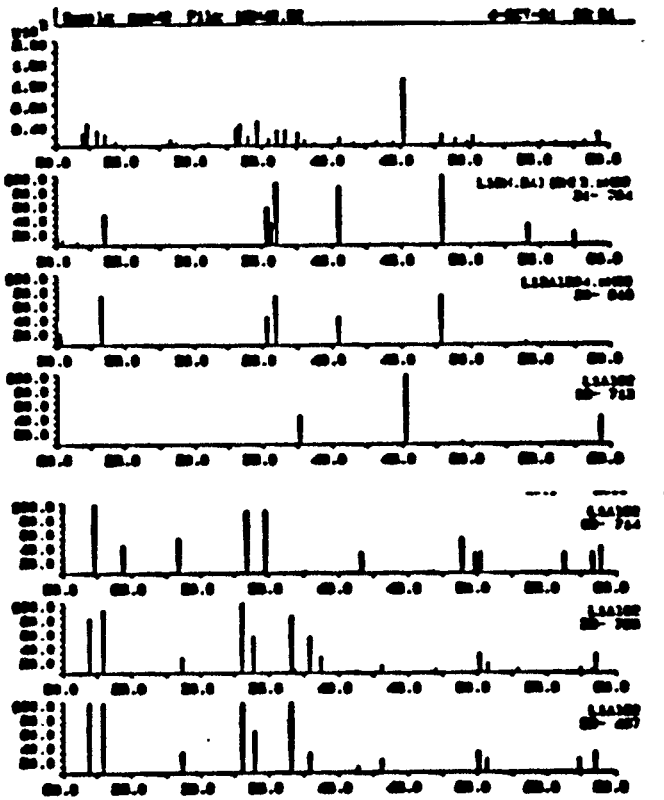

Figure 11 Run 42: Membrane Matrix X-Ray Diffraction Pattern

Run 43

This experimental run was the first successful run which used a completely tape cast membrane MgO matrix. The electrolyte was eutectic potassium/lithium carbonate which was added after the binder material was burned out. Both the cathode and the anode in this experiment started out as lithiated NiO. The process gas for this experiment started out as 1.4% CO_2, 3.9% H_2O, balance methane. Later in the run, 1.38% CO_2, 92 ppm H_2S, 3.9% H_2O, balance methane was used.

The ceramic membrane was manufactured by mixing 16.5 grams MgO, 83.3 grams Metoramics K565-4 Acrylic Binder System (24.9 wt% acrylic polymer), 1 gm Metoramics M-1111 releasing agent, and 1 gm Metoramics M-1114 surfactant. The exact composition of these tape casting agents are proprietary to Metoramics. These were mixed in a ball mill overnight and poured out onto M-1111 coated glass. Air drafts across the surface of the cast were prevented by placing a cardboard sheet over the cast with a 4mm thick spacing between the surface of the cast and the cardboard sheet. This allowed uniform evaporation of the solvents from the cast since the convective effects of room air were minimized. The resulting tape was 42.1 wt% MgO with the remainder acrylic binders. When the binders were burned away, this corresponded to 88.1 vol% free volume.

Three inch diameter, 0.5mm thick membranes were cut from the tape and three of these were layered in the cell. Pure O_2 was blown across the cathode and anode sides of the cell and the assembly was heated to 375°C overnight. The next day, after smoking from the burning binder material was no longer observed, fuel gas (1.40 % CO_2, 3.9% H_2O, balance CH_4) was started to the cathode side of the cell and N_2 was started to the

anode. Electrolyte was added, 20.8 grams, through the reference electrode hole in the top of the cell assembly. Only 17.3 grams were required based on the free volume of the membrane, but more was added to compensate for electrode wetting, wet seal formation with the MACOR housings, and spillage during the adding process.

Upon adding electrolyte to the cell, cross-cell resistance dropped from infinite to 0.35 ohms. Initial tests of the cell performance were centered around CO_2 transport. With applied currents of 400 mA (50.5 mA/cm^2) CO_2 levels dropped from 1.4% to 0.6% (57.1% removal). CO_2 removal data is presented in Figure 12. This corresponds to a current efficiency of only 52%. Since the cross-cell potential was stable at only -1.36 volts, an alternative current path was probably present. Since the CO_2 present in the anode corresponds to the CO_2 removed from the anode to within 75%, there must be transport present by a species that we are not presently analyzing for. This may possibly be explained by the following mechanism:

Cathode:
$$H_2O + Ni \Rightarrow NiO + H_2 \quad (32)$$
$$NiO + 2e^- \Rightarrow Ni + O^{2-} \quad (33)$$

Overall Cathode:
$$H_2O + 2e^- \Rightarrow H_2 + O^{2-} \quad (34)$$

Anode:
$$O^{2-} \Rightarrow 1/2O_2 + 2e^- \quad (35)$$

These two half cell reactions sum to the same overall cell reaction as that for carbonate transport:

$$H_2O \Rightarrow H_2 + 1/2O_2 \quad (36)$$

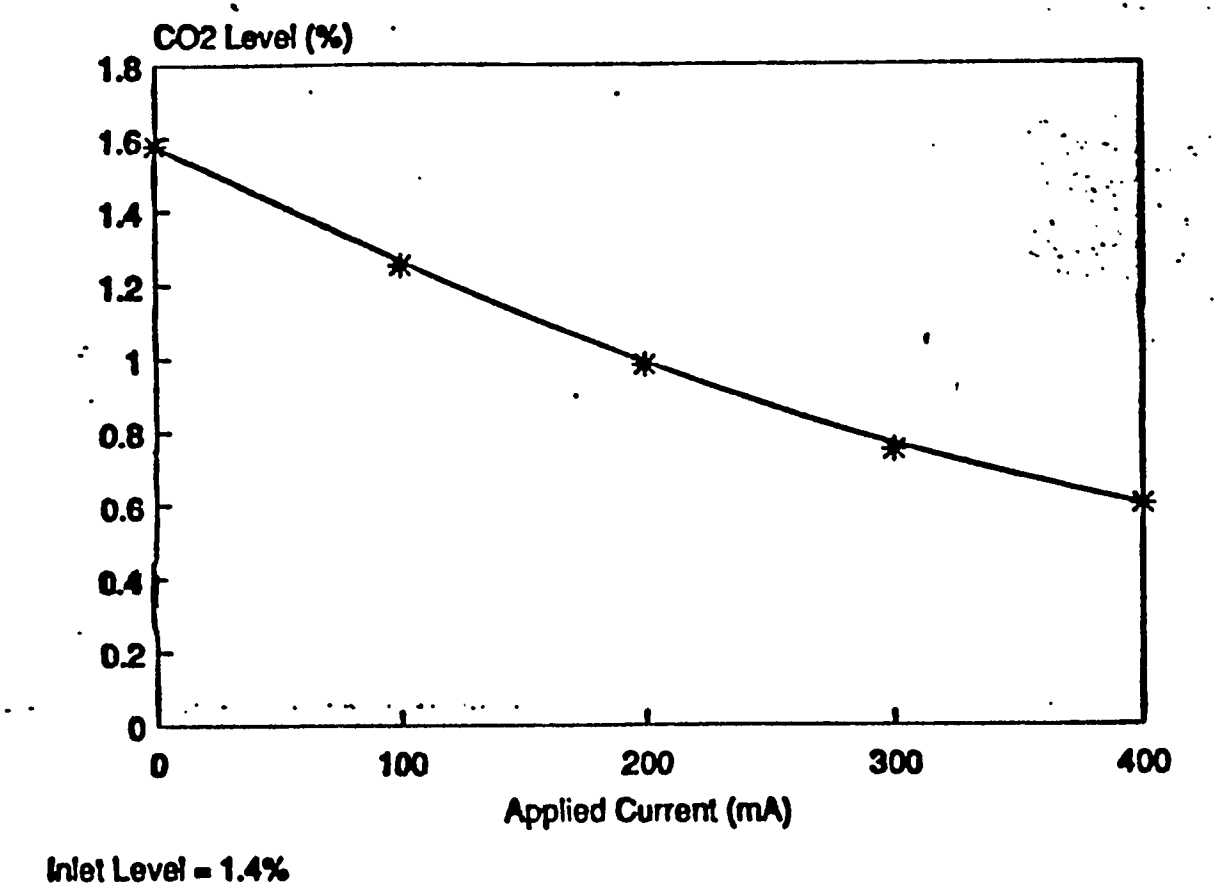

Figure 12 Run 43: CO_2 Level vs Applied Current

The only question is that the O^{2-} ion is highly basic and should react with CO_2 to form CO_3^{2-}. If this were the case, CO_2 would be removed in amounts closer to stoichiometric. This has not been observed. Possible explanations for this lack of CO_2 transport is that the reduction of NiO to Ni in equation (4) takes place below the electrode/electrolyte interface and thus the O^{2-} ion is not exposed to sufficient CO_2 to form appreciable quantities of CO_3^{2-}. Thermodynamic analysis shows that reaction (4) takes place at a standard potential of only -1.596 volts with respect to the O_2/CO_2 reference electrode. Reaction (6) takes place at a standard potential of only 0.773 Volts with respect to the reference electrode (around the same potential as the oxidation of sulfide). Thus the electrochemical potentials for the above mechanism are on the proper order of magnitude.

H_2S was then fed into the system gas by bleeding in a contaminated gas stream to obtain a final gas composition of 1.38% CO_2, 92 ppm H_2S, 3.9% H_2O, and the balance CH_4. Removal was demonstrated to a level of less than 2 ppm with an applied current of 5 mA (current density of 0.63 mA/cm^2) and a process stream flowrate of 415 cc/min. H_2S removal data is presented in Figure 13. This corresponds to 100% current efficiency. It should be noted that nearly 5 days exposure to the H_2S contaminated stream was required to sufficiently sulfide the electrolyte so that any effect with current at all could be seen; current was applied for 24 hours before a sufficient sulfide gradient within the membrane was established to bring cathode process gas concentrations below 2 ppm. At these gas phase concentration levels, the equilibrium sulfide concentration of the

membrane is very slow to be reached as the molar flowrate of sulfide in the gas phase is very small. Cross-cell potentials hovered around -0.650 Volts.

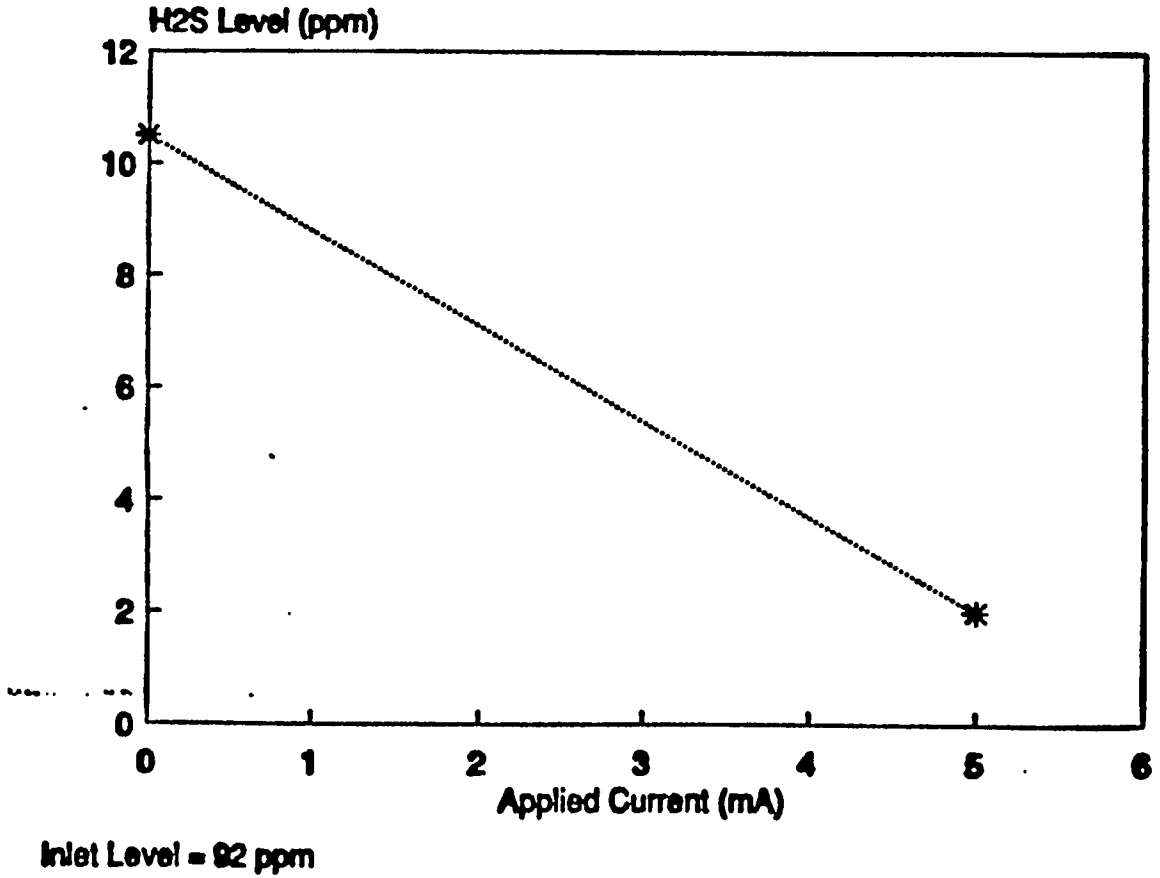

Figure 13 Run 43: H_2S Level vs Applied Current

The cell was shut down after 222 hours of operation when gas supplies ran out. X-ray analysis of the electrode materials showed that the cathode was a mixture of Ni, NiO, Ni_3S_2, and NiS. Cathode X-ray data is presented in Figure 14. The presence of both Ni and NiO in the cathode suggests possible support for the above current transport mechanism through the O^{2-} ion at higher cross-cell potentials. The anode was almost entirely NiO with some traces of Ni present. X-ray data for the anode is presented in Figure 15. Post-run examination of the anode exit gas-flow tube showed a brownish-yellow coating of the interior wall of the tube at a position just outside of the cell furnace. This is the location that condensing sulfur would be expected to collect. The coloration and location of this tube discoloration suggests that it is amorphous sulfur.

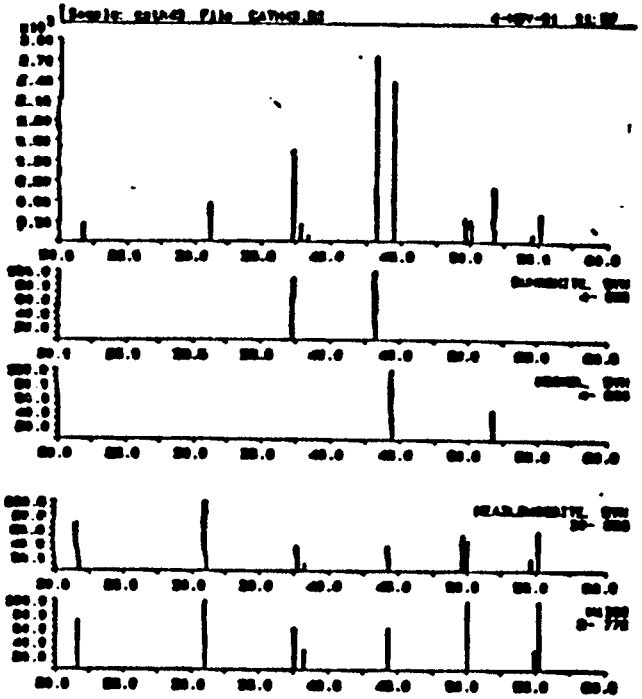

Figure 14 Run 43: Cathode X-Ray Diffraction Pattern

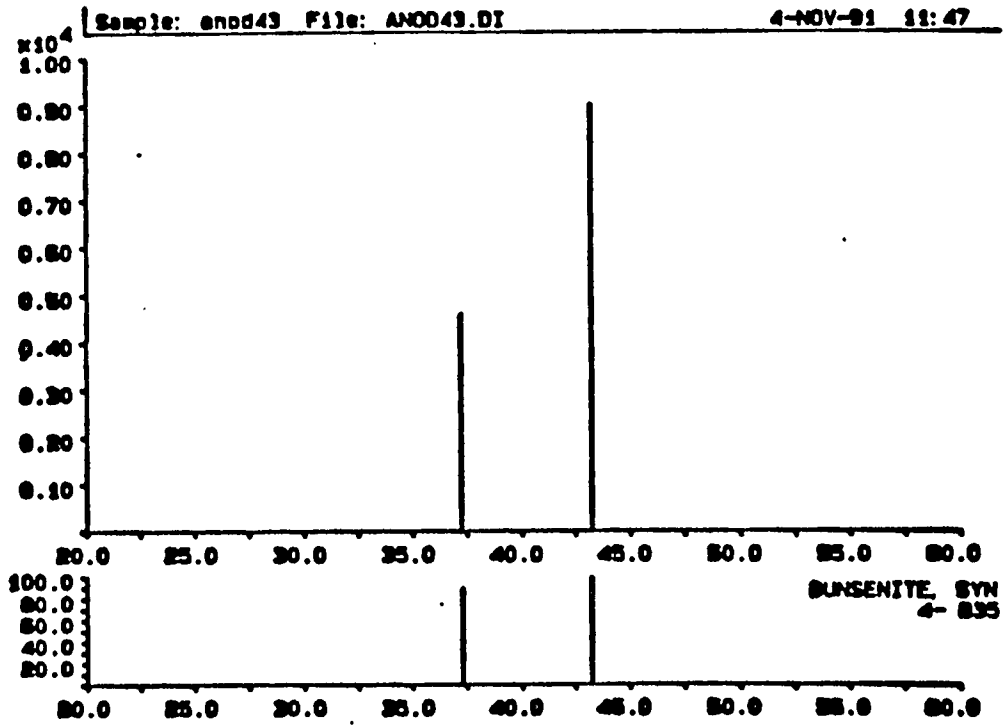

Figure 15 Run 43: Anode X-Ray Diffraction Pattern

Run 49

This was the fifth experimental run using coal gas. It used two tapes of MgO and one mat of zirconia cloth as the membrane matrix material. The electrodes were both lithiated NiO. The acrylic binders in the tapes of MgO were burned out under an O_2 atmosphere and the Li/K eutectic-composition electrolyte was added with the cell at run temperature. MACOR machinable ceramic housings were used instead of stainless steel housings. The inlet gases were passed through a stainless steel shift reactor to allow then to come to their equilibrium composition before passing through the cell.

This experimental run was divided into three sections: the first confirmed ionic transport through the membrane by removal of CO_2 (and H_2O) from the syn-gas at 625°C (Run 49A), the second was an attempt at removal of H_2S from the syn-gas at 625°C (run 49B), and the third was an attempt at removal of H_2S from the syn-gas at 700°C (Run 49C). The results of these studies are presented below:

Run 49A

CO_2 removal from the process gas as a function of applied current was recorded and is presented in Table 2. Examination of this data shows that the removal of CO_2 from the cathode side of the cell and production of CO_2 at the anode side of the cell is stoichiometric across the range of applied currents examined.

Fuel gas flow was set at 75 cc/min and N_2 sweep was set at 63 cc/min. Seals were good and no cross-flow between the two process streams was observed.

Table II.
Run 49A Recorded Data.

Applied Current (mA)	Actual Cathode CO_2 Out	Calc. Cathode CO_2 Out	Actual Anode CO_2 Out	Calc. Anode CO_2 Out
0	17.8%	17.8%	0.0%	0.0%
100	16.8%	16.8%	1.8%	1.2%
200	15.8%	15.7%	2.8%	2.4%
300	15.2%	14.7%	3.8%	3.7%

This data shows that the cell was functioning properly with respect to ionic transport of carbonate through the electrolyte.

After 2.65 hours with current applied, cross-flow between the cathode and the anode was observed, indicating that the ceramic matrix was damaged. Over the next 13.25 hours, 10.5 grams of electrolyte were added to the cell in order to stop this cross-flow by flooding any matrix cracks with electrolyte. Cross-flow between the two process streams was stopped in this manner and H_2S removal with applied current was then examined.

Run 49B

After 22.3 hours exposure to fuel gas at 625°C, an exit H_2S composition of 27.7 ppm was recorded. A current of 5 mA was applied to the cell (0.63 mA/cm^2, superficial electrode area = 7.92 cm^2). After 27.7 hours with applied current, no significant removal of H_2S was observed. Examination of the limiting current densities at these run conditions shows that at 625°C the gas phase limiting current density is only 1.1 mA/cm^2

while the membrane limiting current density is only 1.4 mA/cm^2. This membrane limiting current density assumes as electrolyte diffusivity of 10^{-5} cm^2/sec. Once membrane porosity and tortuosity are taken into account, this estimate is in all probability too large. As an 'order-of-magnitude' estimate, however, it does show that the transport through the membrane is on the same order as the transport through the gas phase. It is probable that at these temperatures, the membrane cannot support the necessary flux of sulfide ion to significantly affect the exit H_2S concentration.

Run 49C

Cell temperature was increased to 700°C. At this temperature, analysis of limiting current densities within the system shows that the gas phase limiting current density is 1.15 mA/cm^2 while the membrane limiting current density is 3.29 mA/cm^2. This shows that even if the electrolyte diffusivity estimate is in error, the membrane flux is three times greater at this temperature than at 625°C. H_2S removal at a variety of flowrates was observed and is tabulated in Table 3. The overpotentials reported here have not been corrected for IR loss. The measured cross-cell resistance by current interrupt was observed to be only around 1Ω. With the maximum current applied to the cell only 20 mA, this corresponds to only 20 mV of ohmic loss. This is negligible compared to the overall cross-cell potential, which includes concentration effects, and potentials required to drive the electrochemical reactions.

Table III.
Run 49C Recorded Data.

Time	Applied Current (mA)	Cathode H_2S Out (ppm)	Cathode - Reference Overpotential	Anode - Reference Overpotential
Cathode flow = 88 cc/min				
17:21 (2/16)	0	85.0	0.0	0.0
18:15	5	26.7	-0.007	0.159
19:48	5	16.0	-0.006	0.127
21:30	0	89.5	0.0	0.0
8:46 (2/17)	0	89.5	0.0	0.0
10:00	5	20.0	-0.030	0.149
12:02	1.2	42.0	N/A	N/A
12:35	2	51.5	-0.017	0.030
13:00	2	47.5	N/A	N/A
13:15	2	53.0	N/A	N/A
13:34	20	29.5	N/A	N/A
14:20	20	9.7	N/A	N/A
14:47	15	18.5	-0.023	0.099
15:07	10	25	-0.022	0.050
15:48	20	15.5	-0.033	0.106

Table III (con.)
Run 49C Recorded Data.

Time	Applied Current (mA)	Cathode H_2S Out (ppm)	Cathode - Reference Overpotential	Anode - Reference Overpotential
Cathode Flow = 210 cc/min				
17:10	0	57	0.0	0.0
18:05	5	35.5	-0.014	0.127
19:00	5	30.6	N/A	N/A
20:09	10	31.5	-0.008	0.213
10:51 (2/18)	0	75.5	0.0	0.0
11:34	5	38.5	0.0	0.184
12:01	5	32	0.003	0.253
12:58	5	30	0.011	0.280
14:23	5	28.5	0.017	0.299
Cathode Flow = 400 cc/min				
21:15	0	59.4	0.0	0.0
21:40	5	48.7	-0.093	0.004
21:55	5	44.5	-0.088	0.055
22:24	5	39.7	-0.081	0.099
22:48	5	39.7	-0.082	0.117
10:31 (2/19)	0	73	0.0	0.0
14:14	10	49	-0.007	0.150
14:55	10	37.3	0.002	0.280
15:34	10	38	0.007	0.293
16:16	15	37.5	0.009	0.333
17:08	15	38.3	0.014	0.343
17:55	20	38.7	0.012	0.326
Cathode Flow = 600 cc/min				
12:00 (2/20)	0	68	0.0	0.0
12:44	10	42	-0.001	0.208
13:15	10	43.3	0.0	0.273
13:45	10	48.3	0.006	0.249
14:30	20	46	0.001	0.318
15:00	20	40	0.003	0.310
15:30	20	45.3	0.003	0.365

The above data are presented graphically in Figures 16 through 19. The H_2S exit composition is plotted against run event for the 88 cc/min data in Figure 16. Note that initially, the membrane was showing process stream cross-flow. 1.5 grams of electrolyte were added to stop the cross flow and 5 mA were applied to the cell. This current level corresponds to five times the theoretical current required for complete H_2S removal. After driving the H_2S down to 16 ppm (81.2% removal, zero current basis) the current was turned off. The exit H_2S level returned to 89.5 ppm. The lowest level to which the H_2S level was driven was 9.7 ppm (89.1% removal, zero current basis). This data shows good response of the system to applied current. The overpotential to accomplish this removal is shown by Figure 20 to be negligible.

The H_2S removal versus run event for the 210 cc/min data is shown in Figure 17. This data still shows good response of the system to applied current. More electrolyte had to be added to repair membrane damage, and thus the initial exit H_2S cathode level with no current applied is down to 57 ppm. This is due to a build-up of carbonate caused by excess electrolyte which had been added to the system.

The data taken at a flowrate of 400 cc/min is presented in Figure 18 and the data taken at 600 cc/min is presented in Figure 19. Comparison of this data with the overpotential results presented in Figure 20 shows that the efficiency of the system dropped off with time. At several points through the run, as marked on Figures 16 through 19, electrolyte was added to stop cross-over between the cathode side of the cell and the anode side. The increase in anodic overpotential shows that this excess electrolyte had flooded the anode, thus decreasing the reactive surface area from the

interfacial area of the electrolyte wetting the walls of the electrode capillaries to the superficial area of the electrode when the pores were fully flooded. This was verified in the post-mortem analysis of the cell when the assembly was taken apart and the components examined. The anode flooded because it is physically on the bottom of the assembly.

A total of 18.7 grams of electrolyte was added to the membrane during the course of the run in addition to the 11 grams that were initially added to fill the ceramic matrix of the membrane. Post-mortem examination of the membrane showed a small fracture in the matrix around the edge of the electrodes. This fracture would be temporarily flooded with electrolyte to form a gas impermeable barrier. However, aggressive attack by the electrolyte on the MACOR housings would deplete the membrane of electrolyte and lead to gas cross-flow. This problem can be overcome by the use of stainless steel housings, which are more resistant to electrolyte attack. The cell was terminated due to flooding of the anode and poor membrane integrity after 216 hours of operation.

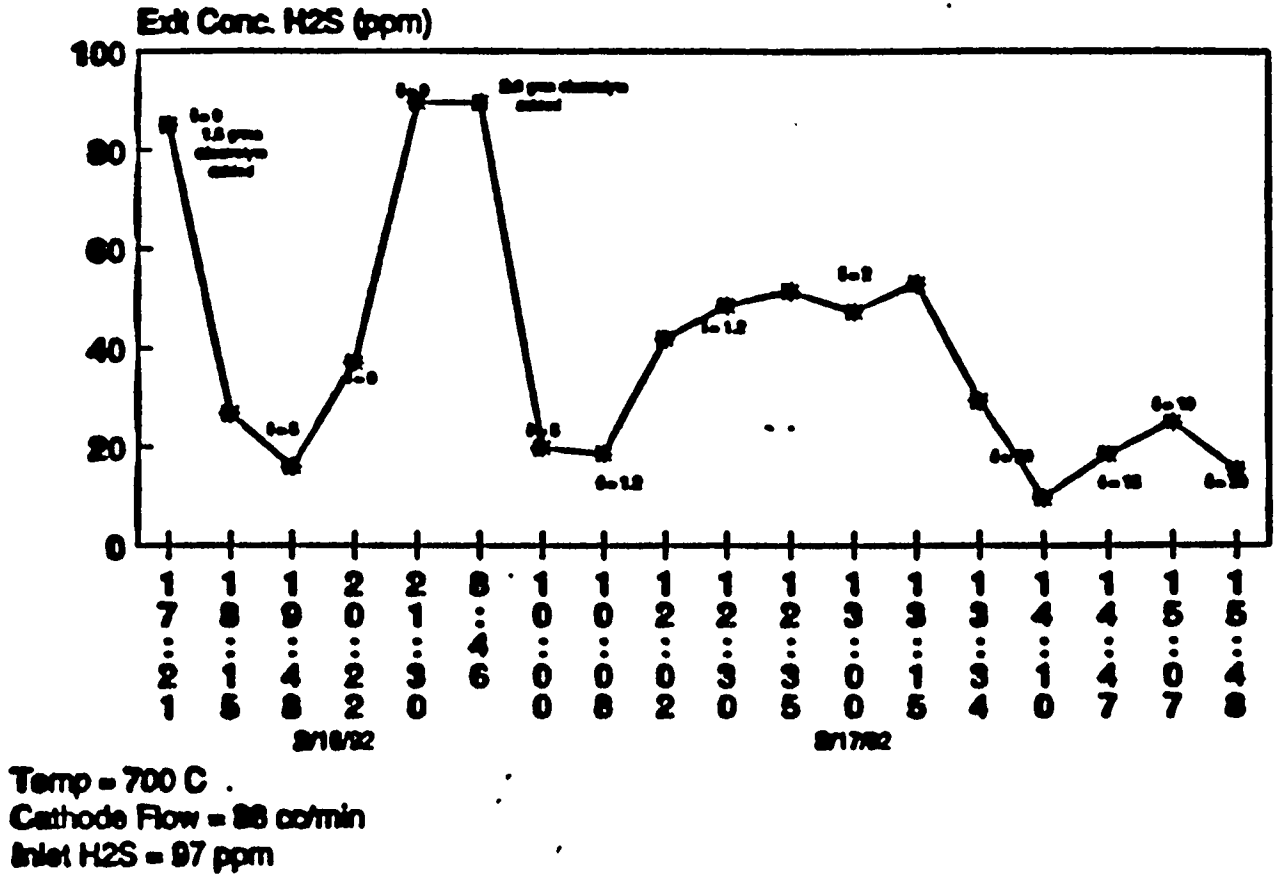

Figure 16 Run 49C: H_2S Concentration vs Applied Current and Time
88 cc/min

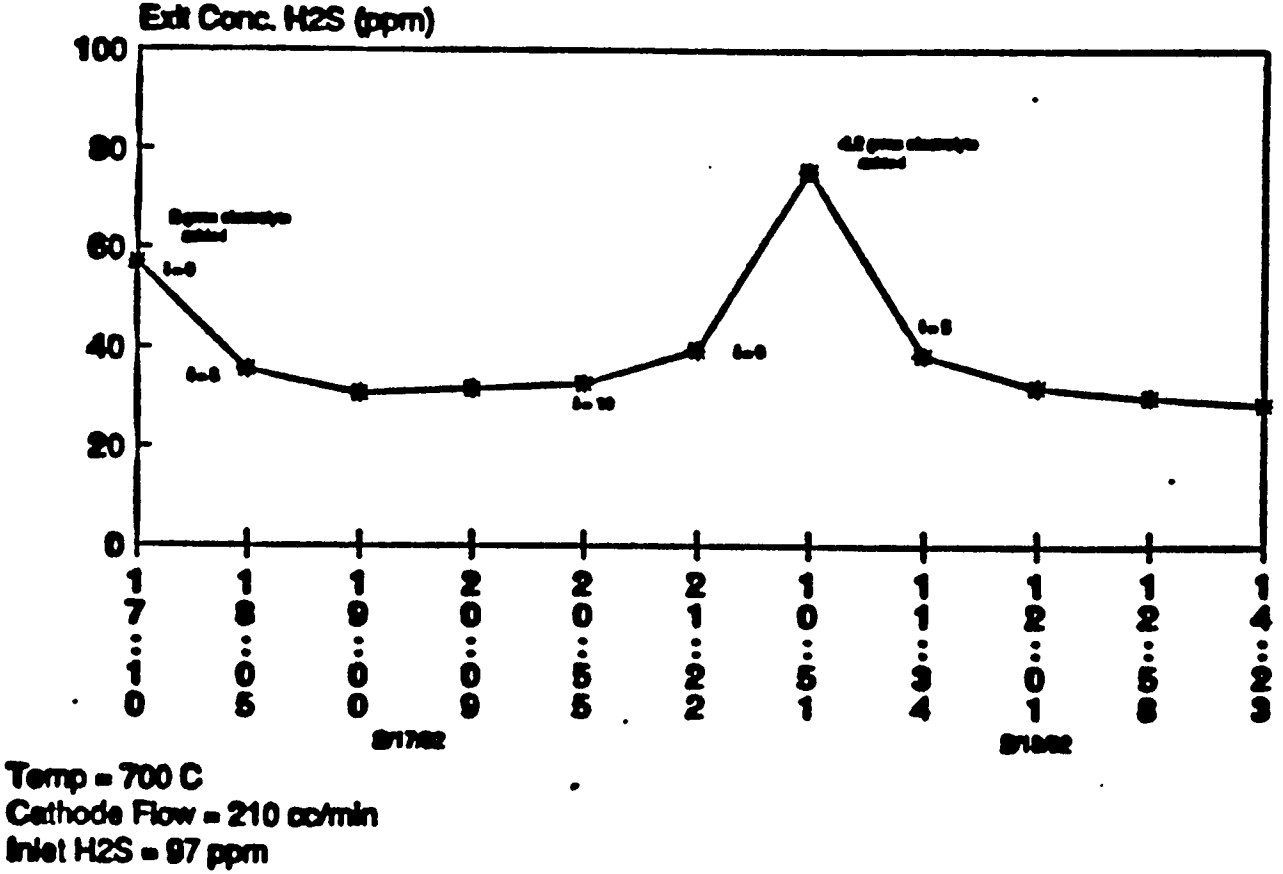

Figure 17 Run 49C: H_2S Concentration vs Applied Current and Time, 210 cc/min

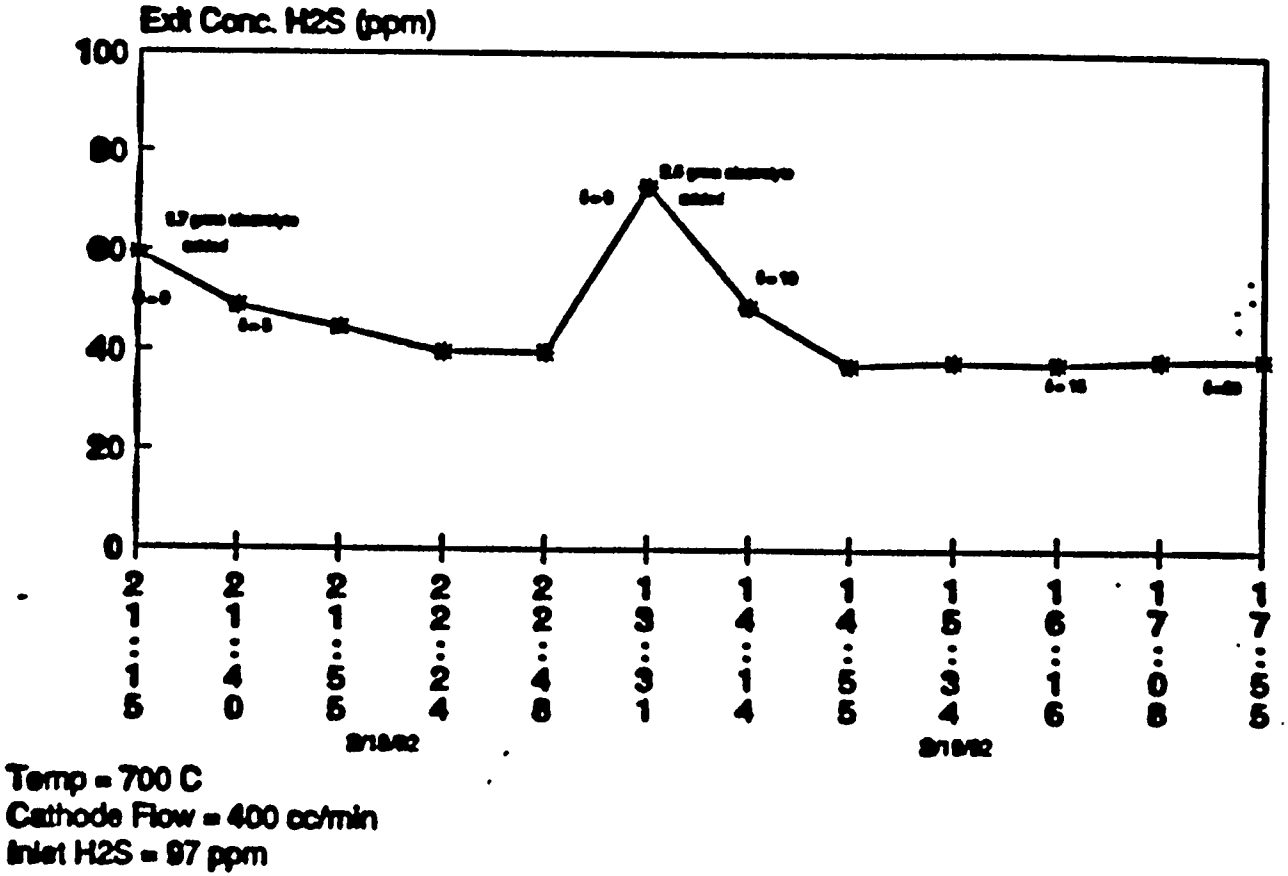

Figure 18 Run 49C: H_2S Concentration vs Applied Current and Time, 400 cc/min

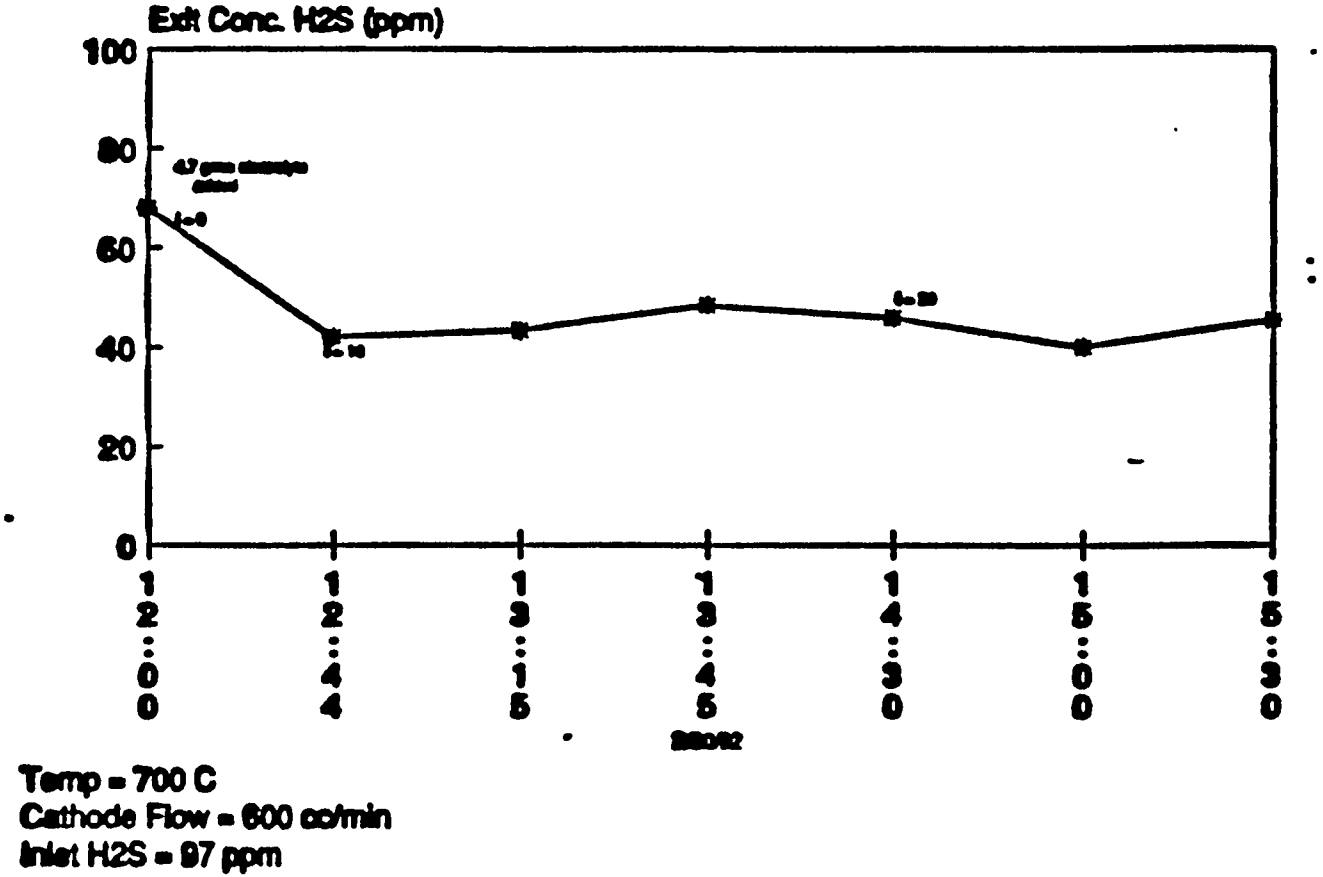

Figure 19 Run 49C: H_2S Concentration vs Applied Current and Time, 600 cc/min

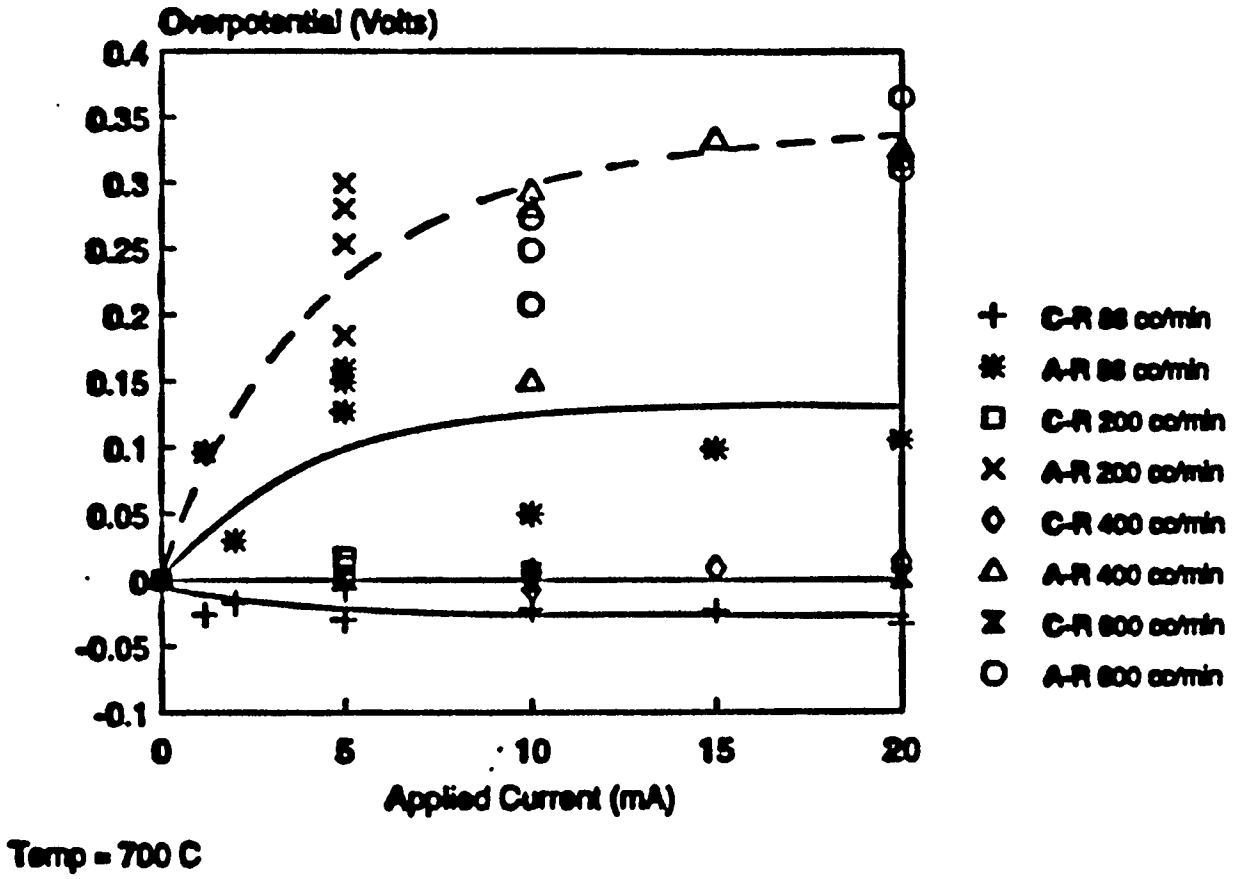

Figure 20 Run 49C: Overpotential vs Applied Current and Time, Various Flow Rates

Run 57

Both electrodes in this experiment were lithiated Ni. The membrane was two tapes of MgO with two mats of zirconia cloth. One of the zirconia mats was cut with a wick extending out of the cell and resting in an electrolyte reservoir. This was to provide a continuous supply of electrolyte to the membrane in the event of electrolyte evaporation/reaction with the cell materials. The electrolyte loaded into the cell was 0.8 mole% sulfide in a carbonate supporting electrolyte. Eutectic carbonate electrolyte was loaded into the reservoir. The cell housings were 316 stainless steel painted with aluminum.

After binder burn-out and the cell had reached run temperature, fuel gas of final composition 14.4%CO_2, 45.1% CO, 6.2% H_2O, 34.2% H_2, and 113 ppmv H_2S was fed to the cell. This gives an equilibrium sulfide level in the electrolyte of 0.63 mole% sulfide. The gas phase limiting current density under these conditions was estimated to be 1.28 mA/cm^2 and the membrane limiting current density was estimated at 1.97 mA/cm^2.

H_2S removal data is presented in Figure 21. Removal of H_2S below 2 ppmv (GC detector limit) was recorded with only 5 mA (0.63 mA/cm^2) applied to the cell and a cross cell potential of only -275 mV (cathode to anode). Upon shutting off applied current, exit H_2S levels only returned to 24 ppm (113 ppm entering the cell). The electrolyte reservoir was removed since it was a potential carbonate sink for reaction with H_2S in the gas. Cell cross flow started soon after this and the cell was shut down. Apparently, electrolyte was wicked out of the membrane onto the surface of the steel housings thereby depleting the membrane of electrolyte and allowing gas cross-over.

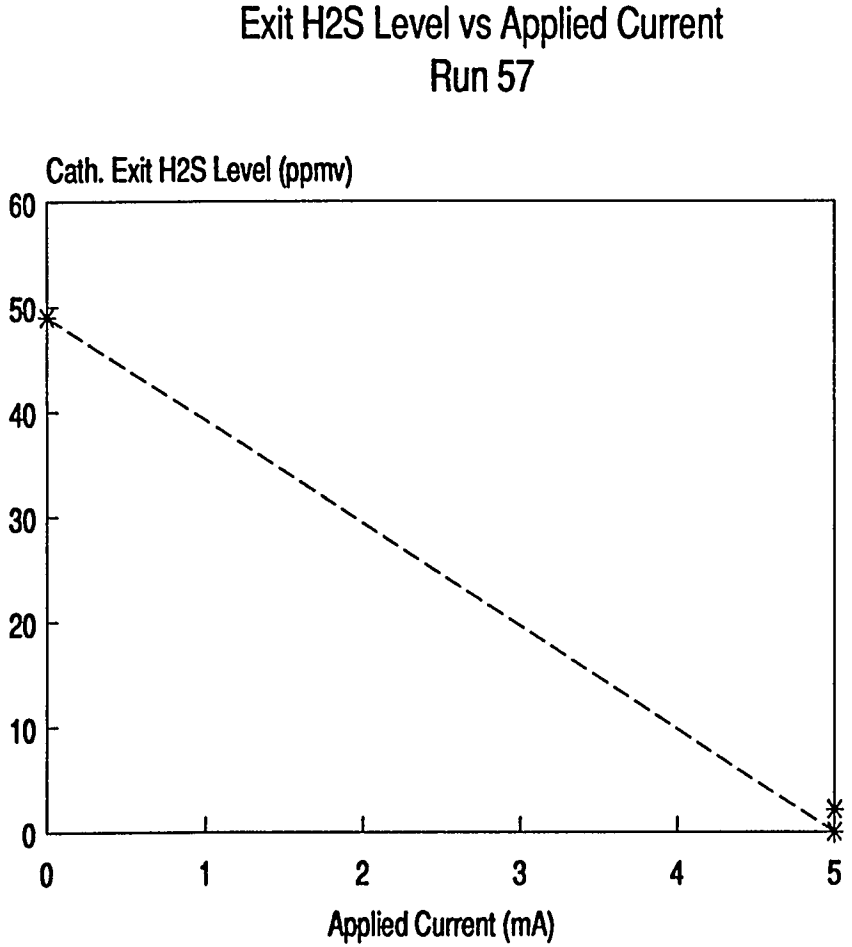

Inlet H2S = 110 ppmv
Cathode Flow = 230 cc/min
Temp = 700 C

Figure 21 Run 57: H_2S Removal vs Applied Current

Run 58

This experimental run also used lithiated Ni electrodes. In this experiment, the membrane was a hot pressed Molten Carbonate Fuel Cell (MCFC) membrane provided by Gas Research Institute (GRI). This structure is a 50/50 weight mixture of $LiAlO_2$ and eutectic Li/K carbonate. The housings were MACOR (with a stainless steel coil in the feed gas line to act as a shift reactor) and aluminum foil gaskets were used. Excess Li_2CO_3 (for reaction with the Al gaskets in conversion to $LiAlO_2$) was sprinkled on the membrane surface with enough Li_2S to bring the electrolyte to 0.8 mole% sulfide.

After the electrolyte was molten, fuel gas with composition 17.3% CO_2, 42.2% CO, 3.3% H_2O, 37.1% H_2, (after shift reaction) and 117 ppmv H_2S was fed to the cell. This gives an equilibrium sulfide level of 0.65 mole%. The calculated gas phase limiting current density at this temperature was found to be 1.31 mA/cm^2 and the membrane limiting current density was estimated to be 1.53 mA/cm^2.

H_2S removal data (see Figure 22), anodic CO_2 production data (see Figure 23), and cross-cell potential data (see Figure 24) was taken. Examination of Figure 22 shows the most dramatic H_2S reduction takes place at currents less than 10 mA (1.23 mA/cm^2). Beyond this, diffusion of H_2 across the cell decreases H_2S current efficiencies in favor of CO_2 production with applied current. Cross-cell potentials were very high at large applied currents (> 500 mA). This was due to concentration effects as the cathode gas was depleted of H_2O by the carbonate transport reaction. H_2S levels were driven as low as 6 ppmv even with H_2 cross-over.

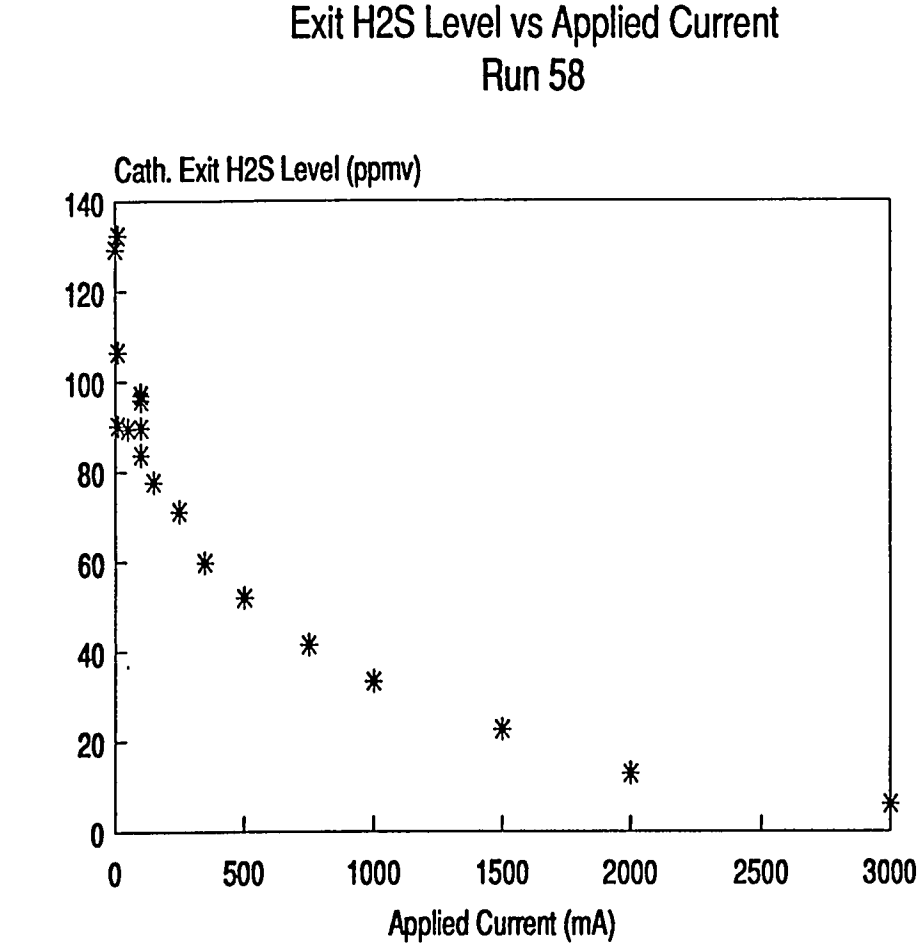

Figure 22 Run 58: H_2S Removal vs Applied Current

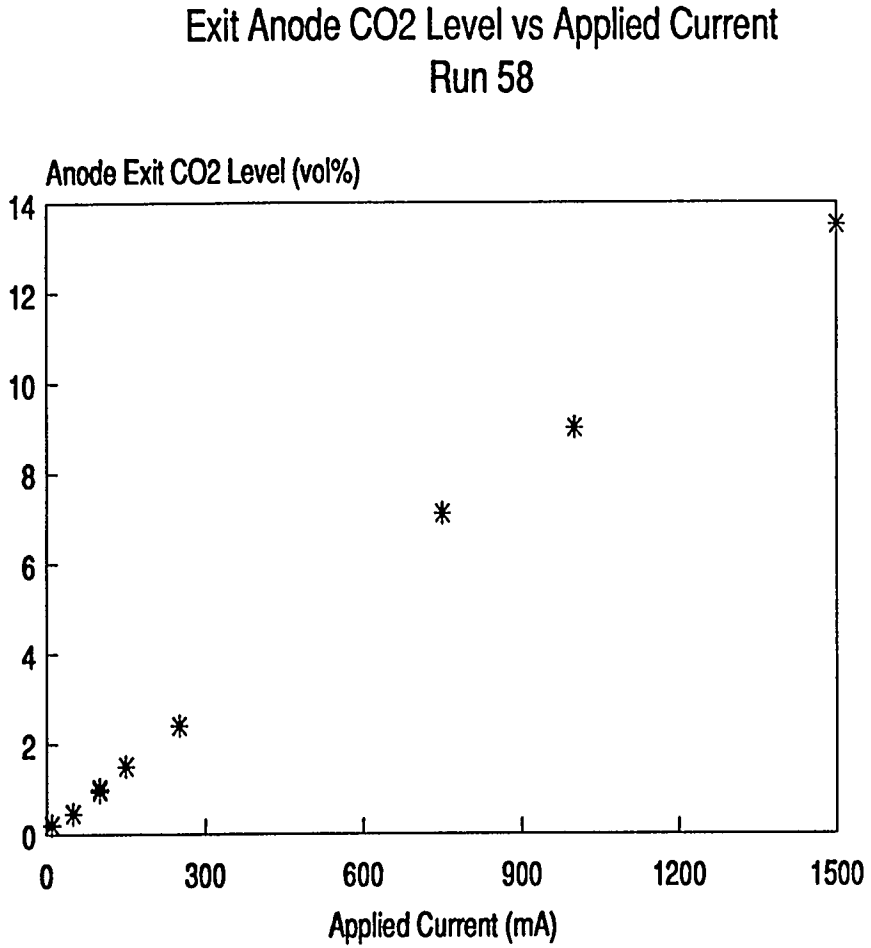

Inlet CO2 = 0 vol%
Anode Flow = 175 cc/min
Temp 700 C

Figure 23 CO_2 Removal vs Applied Current

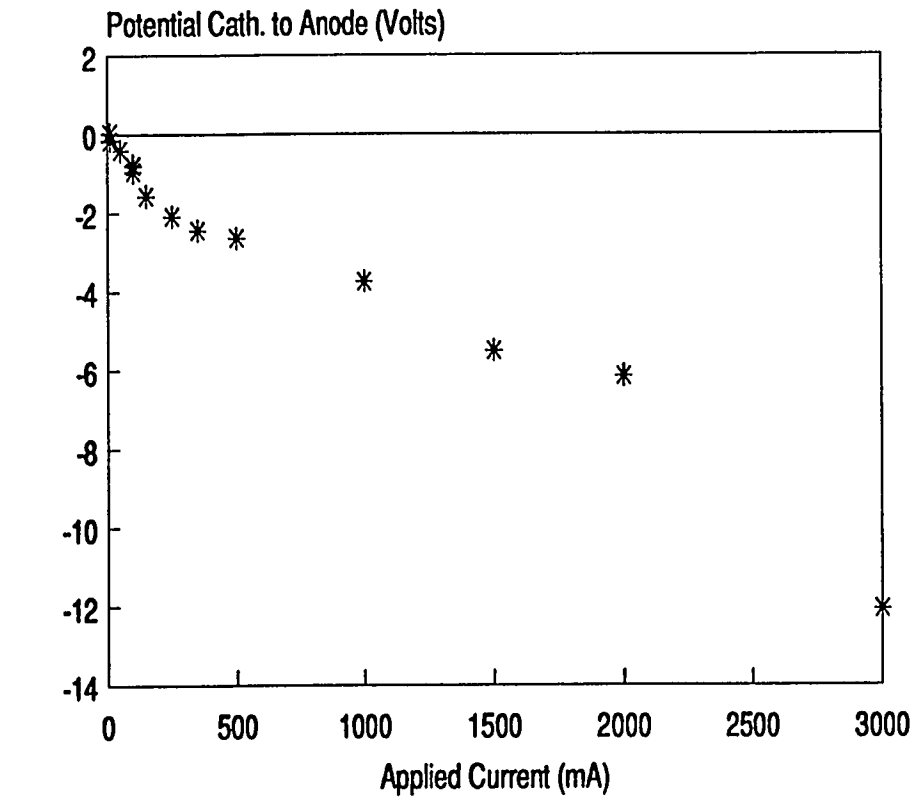

Cathode Flow = 200 cc/min
Anode Flow = 175 cc/min
Temp = 700 C

Figure 24 Run 58: Overpotential vs Applied Current

Run 62

This experimental run used a zirconia mat densified to 64 void %. Only enough electrolyte was added to wet the membrane, extra electrolyte was slowly added after the cell had reached run temperature to react with the Al gaskets.

Once the electrolyte had melted, fuel gas of composition 14.4% CO_2, 45.1% CO, 6.2% H_2O, 34.2% H_2 (after the shift reaction at 700°C) with 120.4 ppmv H_2S. H_2S removal data was taken at 216 cc/min and a temperature of 700°C. At this temperature and gas composition, the equilibrium sulfide level in the electrolyte is calculated to be 0.68%. The gas phase limiting current density is 1.33 mA/cm^2 and the membrane limiting current density is 2.10 mA/cm^2. A second set of H_2S removal data was taken at a flow of 100 cc/min and a temperature of 750°C (gas composition 13.6% CO_2, 45.8% CO, 6.9% H_2O, 33.4% H_2 with 93.6 ppmv H_2S) (see Figures 25 and 26). At this temperature and gas composition, the membrane equilibrium sulfide level was estimated to be 0.91 mole% sulfide. The gas phase limiting current density was estimated to be 1.15 mA/cm^2 and the membrane limiting current density 2.82 mA/cm^2. Anodic CO_2 production was also monitored (see Figures 27 and 28) and cross-cell potentials were recorded for 100 cc/min and run temperature of 750°C (see Figures 29). Comparison of Figures 25 and 26 shows that H_2S removal efficiency is improved by lower flow rates (higher residence time) and higher temperatures (higher limiting current densities).

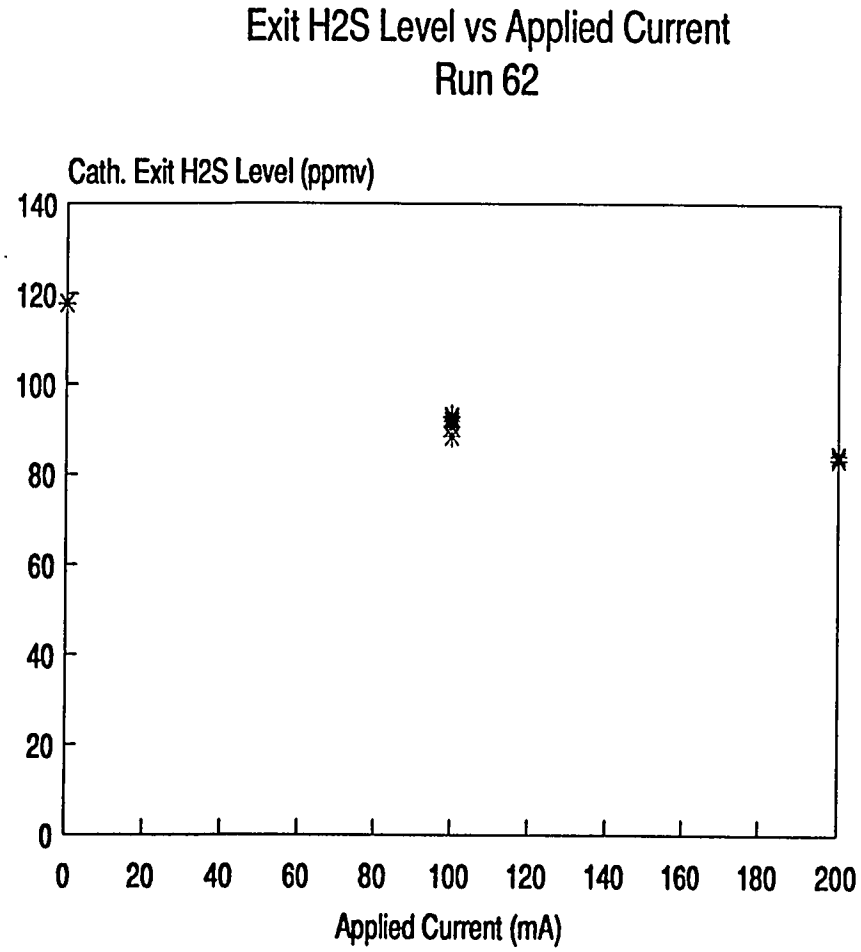

Inlet H2S Level = 120.4 ppmv
Cathode Flow = 216 cc/min
Anode Flow = 42 cc/min

Figure 25 Run 62: H_2S Removal vs Applied Current

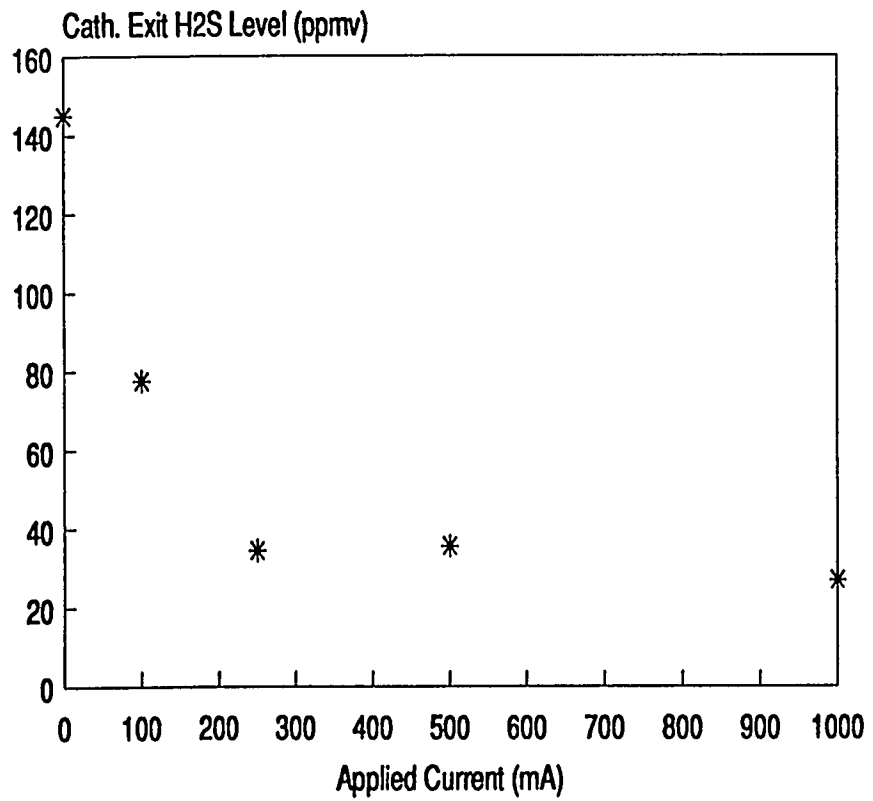

Inlet H2S Level = 93.6 ppmv
Cathode Flow = 100 cc/min
Temp = 750 C

Figure 26 Run 62: H_2S Removal vs Applied Current

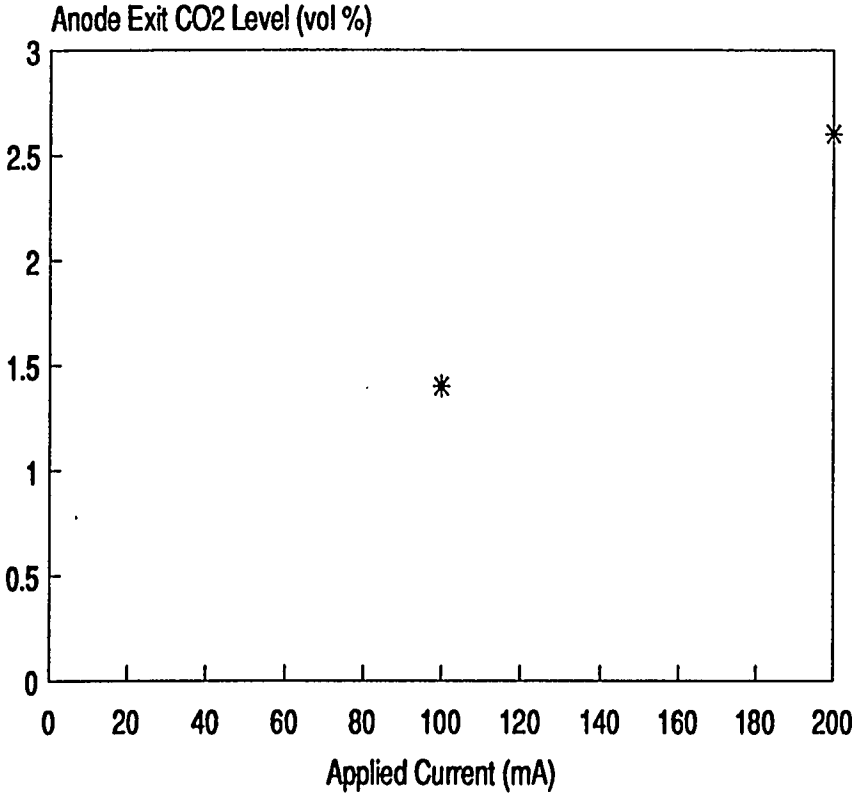

Inlet CO2 Level = 0%
Anode Flow = 42 cc/min
Temp = 700 C

Figure 27 Run 62: CO_2 Removal vs Applied Current

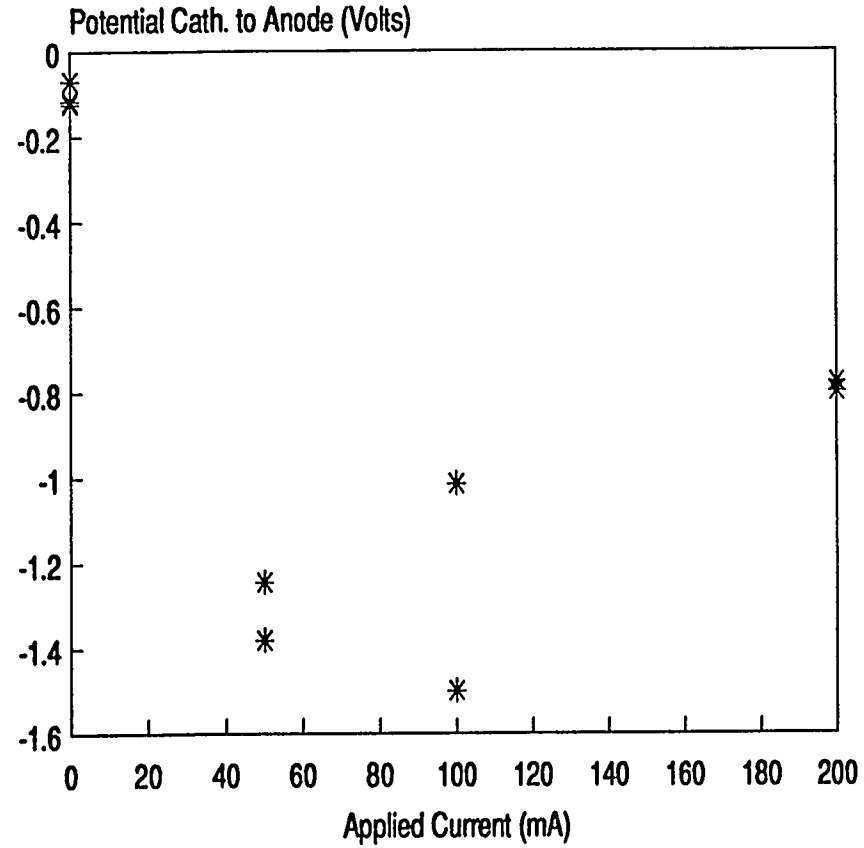

Cathode Flow = 100 cc/min
Anode Flow = 100 cc/min
Temp = 650 C

Figure 28 Run 62: CO_2 Removal vs Applied Current

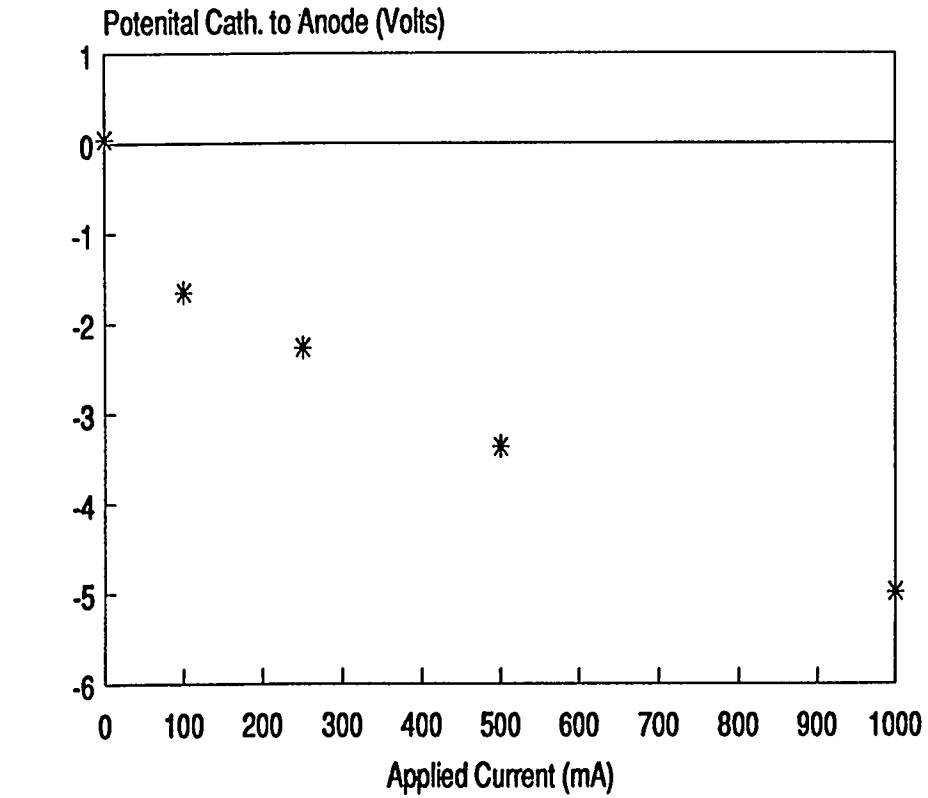

Cathode Flow = 100 cc/min
Anode Flow = 58 cc/min
Temp = 750 C

Figure 29 Run 62: Cross-cell Polarization

Run 65

This experimental run used 1 mat of 30 mil zirconia cloth which was rigidized to 60.8% and two tapes of MgO/ZrO_2 in vinyl binder. The electrolyte was eutectic carbonate and was added to the cell as a pressed disk. the electrodes were lithiated Ni. The housings were MACOR and Al foil gaskets were used. The run temperature was 650°C.

After binder burnout and electrolyte melting, fuel gas of composition 15.2% CO_2, 44.2% CO, 5.4% H_2O, 35.0% H_2 with 18.8 ppmv H_2S was put through the cell. This gas composition and temperature gives an equilibrium membrane sulfide level of 0.06 mole% sulfide. The gas phase limiting current density is estimated to be 0.18 mA/cm^2 and the membrane limiting current density is 0.34 mA/cm^2.

H_2S removal data was taken at cathodic flow rates of 200 cc/min and 100 cc/min (see Figures 30 and 31). Cell polarization data was also take at these flow rates (see Figures 32 and 33). Anodic CO_2 production data was also taken at cathodic flow of 100 cc/min (see Figure 34).

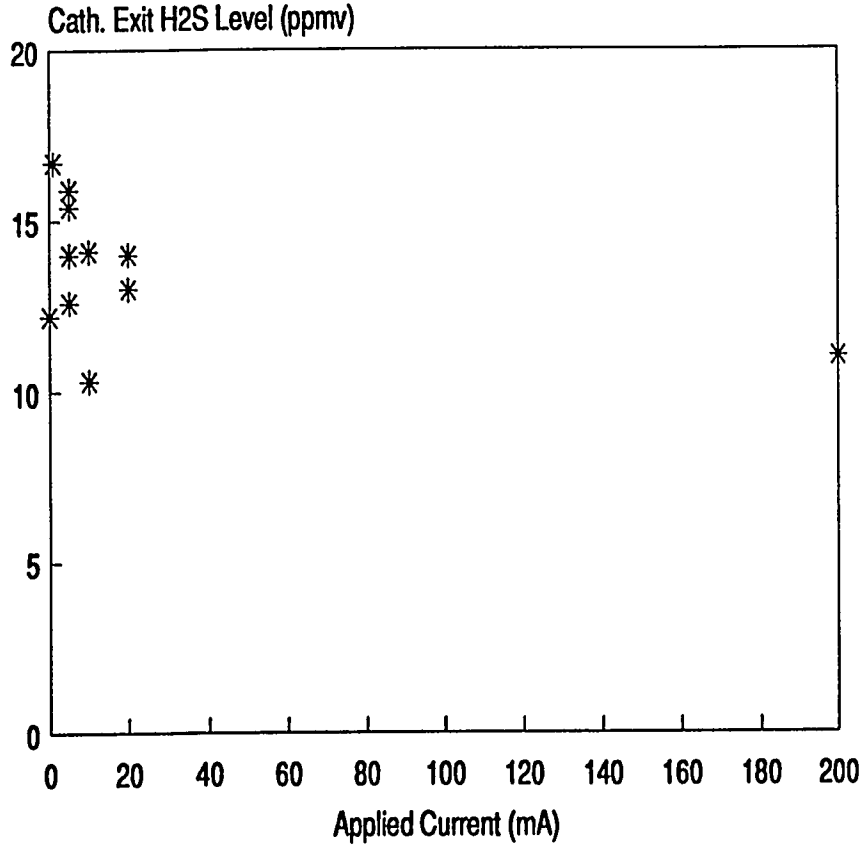

Inlet H2S Level = 18.8 ppmv
Cathode Flow = 200 cc/min
Temp = 650 C

Figure 30 Run 65: H_2S Removal vs Applied Current

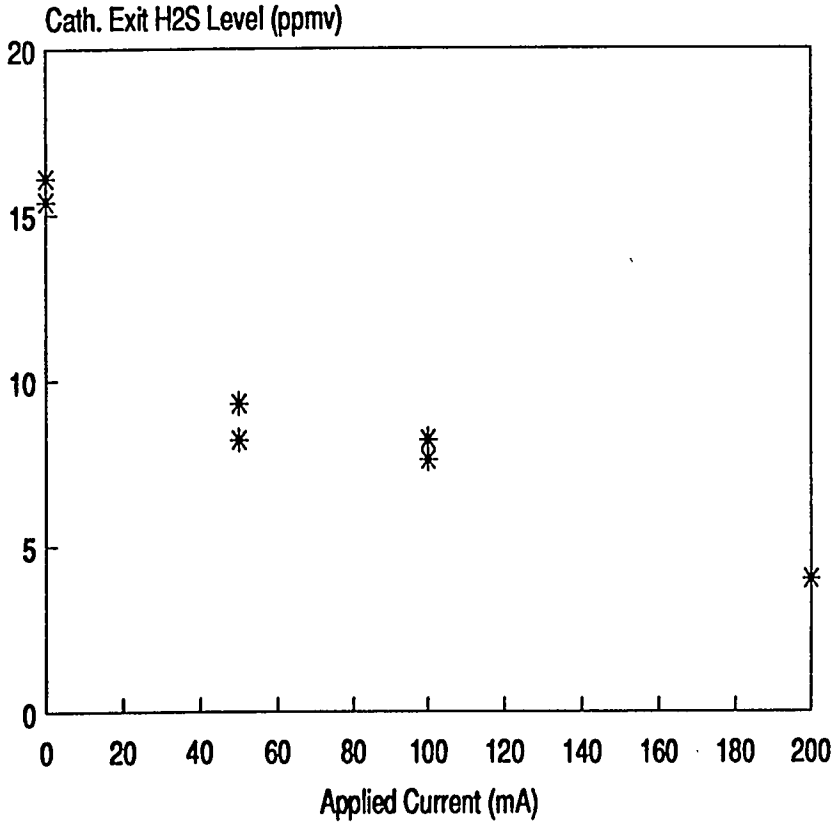

Inlet H2S = 27 ppmv
Cathode Flow = 100 cc/min
Temp = 650 C

Figure 31 Run 65: H_2S Removal vs Applied Current

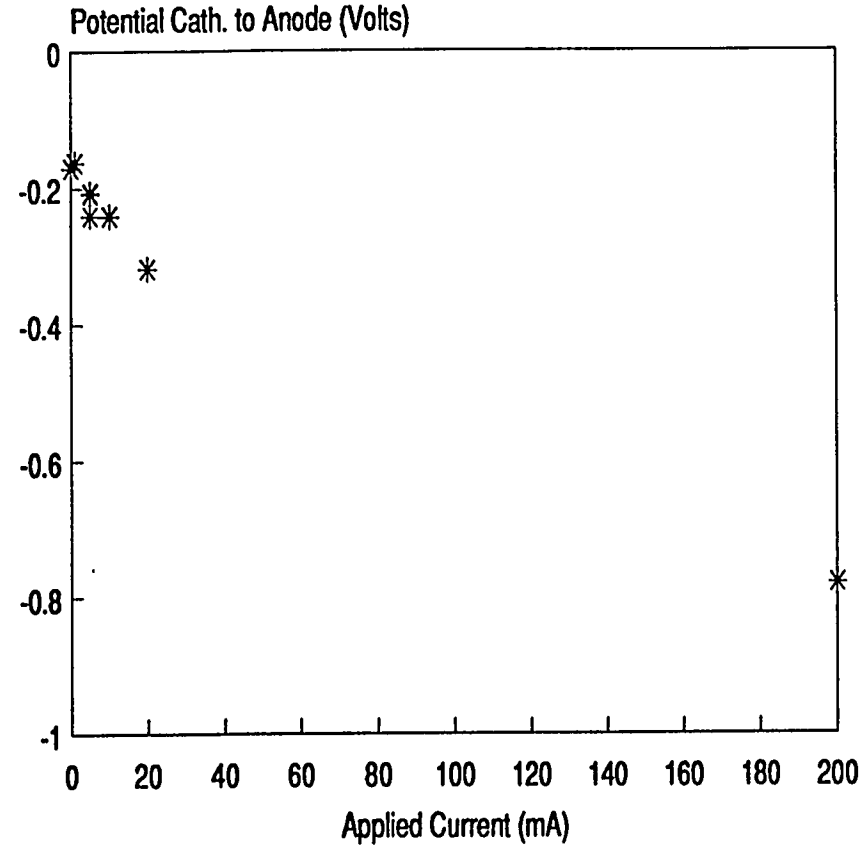

Cathode Flow = 200 cc/min
Anode Flow = 100 cc/min
Temp = 650 C

Figure 32 Run 65: Cross-cell Polarization

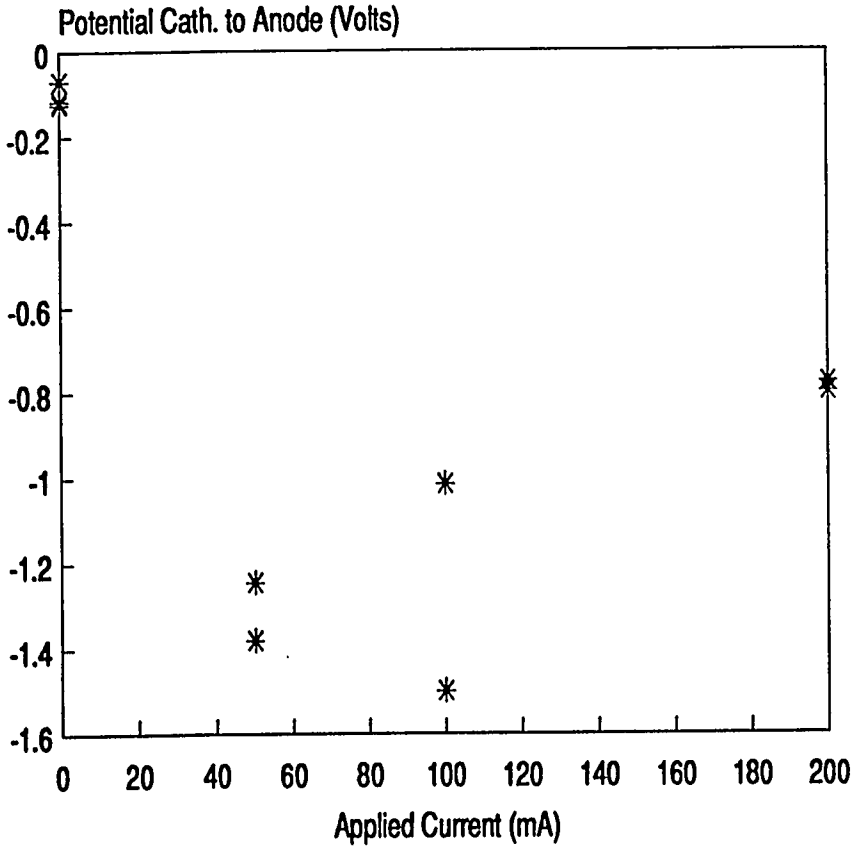

Cathode Flow = 100 cc/min
Anode Flow = 100 cc/min
Temp = 650 C

Figure 33 Run 65: Cross-cell Polarization